Co-delivery of docetaxel and gemcitabine by anacardic acid modified self-assembled albumin nanoparticles for effective breast cancer management

Kushwah, V., Katiyar, S. S., Dora, C. P., Kumar Agrawal, A., Lamprou, D. A., Gupta, R. C., & Jain, S. (2018). Co-delivery of docetaxel and gemcitabine by anacardic acid modified self-assembled albumin nanoparticles for effective breast cancer management. *Acta Biomaterialia*, *73*, 424-436. https://doi.org/10.1016/j.actbio.2018.03.057

Published in:
Acta Biomaterialia

Document Version:
Peer reviewed version

Queen's University Belfast - Research Portal:
Link to publication record in Queen's University Belfast Research Portal

Publisher rights
Copyright 2018 Elsevier.
This manuscript is distributed under a Creative Commons Attribution-NonCommercial-NoDerivs License (https://creativecommons.org/licenses/by-nc-nd/4.0/), which permits distribution and reproduction for non-commercial purposes, provided the author and source are cited.

General rights
Copyright for the publications made accessible via the Queen's University Belfast Research Portal is retained by the author(s) and / or other copyright owners and it is a condition of accessing these publications that users recognise and abide by the legal requirements associated with these rights.

Take down policy
The Research Portal is Queen's institutional repository that provides access to Queen's research output. Every effort has been made to ensure that content in the Research Portal does not infringe any person's rights, or applicable UK laws. If you discover content in the Research Portal that you believe breaches copyright or violates any law, please contact openaccess@qub.ac.uk.

Open Access
This research has been made openly available by Queen's academics and its Open Research team. We would love to hear how access to this research benefits you. – Share your feedback with us: http://go.qub.ac.uk/oa-feedback

Download date:28. Apr. 2024

Elsevier Editorial System(tm) for Acta Biomaterialia

Manuscript Draft

Manuscript Number: AB-17-2575R2

Title: Co-delivery of docetaxel and gemcitabine by anacardic acid modified self-assembled albumin nanoparticles for effective breast cancer management

Article Type: Full length article

Keywords: Combination chemotherapy; Self-assembled nanoparticle; Targeted drug delivery; Biodistribution; DMBA breast cancer model; Drug-polymer conjugate.

Corresponding Author: Dr. Sanyog Jain, Ph.D.

Corresponding Author's Institution: Centre for Pharmaceutical Nanotechnology, Department of Pharmaceutics, National Institute of Pharmaceutical Education and Research (NIPER), SAS Nagar (Mohali) 160062, Punjab, India

First Author: Varun Kushwah

Order of Authors: Varun Kushwah; Sameer S Katiyar; Chander P Dora; Ashish K Agrawal; Dimitrios A Lamprou; Ramesh C Gupta; Sanyog Jain, Ph.D.

Abstract: In the present study, we have modified bovine serum albumin (BSA) by covalently conjugating with anacardic acid (AA) and gemcitabine (GEM) and further used for development of docetaxel (DTX) loaded nanoparticles (AA-GEM-BSA NPs). AA is supposed to provide tumor targeting through VEGF receptors overexpressed in tumors, while the combination of GEM and DTX is supposed to provide synergistic activity by targeting multiple pathways. The conjugate was synthesized via carbodiimide chemistry and characterized by 1H NMR, FTIR, MALDI-TOF and elemental analysis. Conformational changes owing to conjugation of AA and GEM were estimated via fluorescence, Raman and CD spectroscopy, while changes in physiochemical properties were studied by differential scanning calorimetry (DSC), thermogravimetry (TGA) and contact angle goniometry (CAG). Synthesized conjugate was further transformed into DTX loaded NPs and freeze dried. Scanning Electron Microscopy (SEM) and Atomic Force Microscopy (AFM) demonstrated formation of spherical NPs having particle size, 163±8 nm, PDI, 0.13±0.09 and ZP, -27±1 mV. Cellular uptake in MCF-7 and MDA-MB-231 revealed hNTs, OATP1B3 independent, clathrin mediated internalization followed via nuclear co-localization of C-6 loaded AA-GEM-BSA NPs, responsible for significantly higher apoptosis index. Pharmacokinetic profile of DTX loaded AA-GEM-BSA NPs revealed 6.12 and 3.27-fold and 6.28 and 8.9-fold higher AUC and T1/2 values of DTX and GEM as compared to Taxotere® and Gemzar®, respectively. Interestingly, the developed NPs were found safe with no marked effect on RBCs, lower hepato and nephro toxicity. Data in hand suggest promising potential of developed NPs in ameliorating the pharmacokinetic and therapeutic profile of combinatorial regimen of DTX and GEM.

To,
The Editor-in-chief,
Acta Biomaterialia.
Sub: Submission of revised manuscript
Dear Sir,
Please find enclosed herewith our research article entitled **"Co-delivery of docetaxel and gemcitabine by anacardic acid modified self-assembled albumin nanoparticles for effective breast cancer management"** for favor of publication in your esteemed journal. We have thoroughly gone through editor's and reviewer's comments and revised the manuscript accordingly. We appreciate the time and detail provided by you and reviewer's and have incorporated the suggested changes into the manuscript to the best of my ability. The manuscript has certainly benefited from these insightful revision suggestions.

Thus, I request to please accept the revised manuscript and response sheet for further consideration. Moreover, the paper has been prepared according to the guidelines of the journal. I certify that this manuscript, or any part of it, has not been published and will not be submitted elsewhere for publication while being considered by the Acta Biomaterialia.

Kindly acknowledge the receipt of the same.

Thanks and regards,
Sincerely,
[Dr. Sanyog Jain]
Associate Professor
Centre for Pharmaceutical Nanotechnology, Department of Pharmaceutics,
National Institute of Pharmaceutical Education and Research (NIPER)
Sector 67, S.A.S. Nagar (Mohali); Punjab 160062 India

Response Sheet

Authors thank the editor and reviewers for providing constructive comments/suggestions that helped us to further improve the manuscript. We have provided detailed response to each comment and revised the manuscript accordingly.

Editor's comments to authors:

In addition to the remaining comments from Reviewer #4, please address the following:

Comment 1: Please remove highlighting in the Supplementary Materials as that section is not copy-edited, as is outlined in our Guide for Authors, and will appear as is.
Response: The highlighting is now removed in the revised Supplementary Material.

Comment 2: The issue with your use of significant digits persists throughout the body of the manuscript and the tables. The Editor asks once again that you please evaluate your use of significant digits. Please consult the following link from the University of Texas for a helpful explanation: gsspc.cm.utexas.edu/AISD/SignificantDigitsAndStandardDeviation.doc If you have difficulties with downloading this document, please don't hesitate to reach out to our office. Just a few examples:
- Table 2: 24295.4±533.8 should be 24300±534; 36.50±1.9 should be 37±2,
- Table 1: 9.06±6.31 should be 9±6,
- The Abstract: -26.5±1.27 should be -27±1,
- The body of the manuscript: -34.5±1.65 should be -35±2.

There are many such instances throughout the manuscript.
Response: Authors apologize for not mentioning the significant digits. Authors have revisited the manuscript and the significant digits are now appended in the revised manuscript.

Reviewer #4:

Comment 1: The revised manuscript has certain improvement. However, for comment 5 "In vivo antitumor efficacy, Figure 8C. All the morphology of the tumors which extracted from the sacrificed mice at the end of experiment must be listed. The data made the in vivo antitumor efficacy of cancer therapy would be more convinced and visible." The authors did not give the satisfied response.

As description in the section of 2.2.9 In vivo antitumor efficacy. "Once the average tumor volume reached about 100 mm3, tumor bearing animals were separated and randomly divided into different groups each containing 5 animals." At the end of the in vivo antitumor efficacy experiment, all of the morphology of the tumors which extracted from the sacrificed mice should be provided.

Response: As per reviewer's suggestion, the morphology of the tumors extracted from the sacrificed animals is appended in the revised manuscript.

*Manuscript File
Click here to view linked References

Co-delivery of docetaxel and gemcitabine by anacardic acid modified self-assembled albumin nanoparticles for effective breast cancer management

Varun Kushwah[1,2,3], Sameer S. Katiyar[1], Chander Parkash Dora[1], Ashish Kumar Agrawal[2], Dimitrios A. Lamprou [3,4], Ramesh C. Gupta[2], Sanyog Jain[1]*

[1]Centre for Pharmaceutical Nanotechnology, Department of Pharmaceutics, National Institute of Pharmaceutical Education and Research, SAS Nagar, Punjab, India.

[2]James Graham Brown Cancer Centre, University of Louisville, Louisville, KY, USA.

[3]Strathclyde Institute of Pharmacy & Biomedical Sciences (SIPBS), University of Strathclyde, Cathedral Street, Glasgow, G4 0RE, United Kingdom.

[4]Medway School of Pharmacy, University of Kent, Medway Campus, Anson Building, Central Avenue, Chatham Maritime, Chatham, Kent, ME4 4TB, United Kingdom.

*To whom correspondence should be addressed: E-mail: sanyogjain@niper.ac.in, sanyogjain@rediffmail.com, Tel.: +91-172-2292055, Fax: +91-172-2214692

Abstract

In the present study, we have modified bovine serum albumin (BSA) by covalently conjugating with anacardic acid (AA) and gemcitabine (GEM) and further used for development of docetaxel (DTX) loaded nanoparticles (AA-GEM-BSA NPs). AA is supposed to provide tumor targeting through VEGF receptors overexpressed in tumors, while the combination of GEM and DTX is supposed to provide synergistic activity by targeting multiple pathways. The conjugate was synthesized via carbodiimide chemistry and characterized by ^{1}H NMR, FTIR, MALDI-TOF and elemental analysis. Conformational changes owing to conjugation of AA and GEM were estimated *via* fluorescence, Raman and CD spectroscopy, while changes in physiochemical properties were studied by differential scanning calorimetry (DSC), thermogravimetry (TGA) and contact angle goniometry (CAG). Synthesized conjugate was further transformed into DTX loaded NPs and freeze dried. Scanning Electron Microscopy (SEM) and Atomic Force Microscopy (AFM) demonstrated formation of spherical NPs having particle size, 163±8 nm, PDI, 0.13±0.09 and ZP, -27±1 mV. Cellular uptake in MCF-7 and MDA-MB-231 revealed hNTs, OATP1B3 independent, clathrin mediated internalization followed via nuclear co-localization of C-6 loaded AA-GEM-BSA NPs, responsible for significantly higher apoptosis index. Pharmacokinetic profile of DTX loaded AA-GEM-BSA NPs revealed 6.12 and 3.27-fold and 6.28 and 8.9-fold higher AUC and $T_{1/2}$ values of DTX and GEM as compared to Taxotere® and Gemzar®, respectively. Interestingly, the developed NPs were found safe with no marked effect on RBCs, lower hepato and nephro toxicity. Data in hand suggest promising potential of developed NPs in ameliorating the pharmacokinetic and therapeutic profile of combinatorial regimen of DTX and GEM.

Key words: Combination chemotherapy, Self-assembled nanoparticle, Targeted drug delivery, Biodistribution, DMBA breast cancer model, Drug-polymer conjugate.

1 INTRODUCTION

Combination therapy with two or more drugs has emerged as a promising approach for the synergistic therapeutic efficacy and to suppress the cancer drug resistance, as different drug molecules can exert their therapeutic effects at different stages of the growth cycles, leading to synergistic anticancer response.[1] In addition, it also overcome the deleterious adverse effects associated with higher doses of individual drugs by enhancing the therapeutic efficiency via multi-facet pharmacodynamics actions.[2] Among the various combination regimens, Docetaxel (DTX) and Gemcitabine (GEM) is well tolerated and is found to be efficient as first-line therapy for advanced, metastatic non-small-cell lung, metastatic uterine leiomyosarcoma and metastatic breast cancer.[3-5]

GEM is an inactive analogue of nucleoside deoxycytidine, which upon intracellular phosphorylation yields the di- and triphosphate active moieties, that inhibit ribonucleotide reductase and integrates into DNA, leading to the termination of DNA synthesis.[6] Whereas, DTX functions by stabilizing tubulin and induces phosphorylation of bcl-2, promoting apoptosis which results in inhibition of mitotic and interphase arrest.[7] GEM is highly hydrophilic in nature (water solubility of ~83 mg/ml), with a short $T_{1/2}$ (half-life of 32–84 min) and rapidly decomposed into its inactive uracil metabolite (2′-deoxy-2′,2′-difluorouridine (dFdU)), which accounts for up to 99% of metabolic product.[8] Consequently, frequent higher doses of GEM have to be administered to achieve the therapeutic level, which leads to enhanced dose dependent toxicity. While, DTX is highly hydrophobic with very less water solubility and DTX formulation for clinical application (Taxotere®) consists of a 40 mg/ml of DTX in a vehicle composed of high concentration of Tween 80® as solubilizer and ethanol as co-solvent, which results into severe anaphylactic (hypersensitivity) toxicity and even death.[9] In order to decrease undesired side

effects due to polysorbate 80, all patients have to be treated with dexamethasone 3 days prior to the treatment, which leads to compromised immune response in patients.[10] Because of these side effects, patient dropout rate of docetaxel therapy is quite high by the end of second/third treatment cycle. Some formulation strategies have been reported to circumvent the problems of individual drug.[11, 12] According to Wei, star-shaped mannitol-core PLGA-TPGS diblock copolymer and polydopamine-based surface modification of novel NPs-aptamer bioconjugates showed promising potential in elevating the anti-cancer efficacy of DTX.[13, 14] However, the studies were carried out with single drug and no combinatorial drug delivery system has been employed. Nevertheless, few reports of liposomal based nanoformulation for combination therapy of DTX and GEM were published. According to Liang et al. and Yang et al, the liposomal formulation demonstrated higher in vitro and in vivo therapeutic efficacy.[15, 16] However, the formulations demonstrated higher release pattern of GEM within 24 h owing to its hydrophilic nature. Moreover, the reports did not address the deliverability and pharmacokinetic of drugs having extremely different physicochemical properties, which are still the major hurdles of combination therapy.

In the present study, we hypothesize that the poor physicochemical properties of the GEM can be fruitfully modified by conjugating it with albumin protein. The polymeric conjugate of the GEM-albumin could increase drug stability against deamination from cytidine deaminase (CDA) resulting in enhanced plasma half-life of the drug.[17] But upon conjugation of GEM, the hydrophilicity of albumin would remarkably increase which reduces the affinity towards DTX. Thus, to regain the hydrophobic and hydrophilic balance of albumin, hydrophobic anacardic acid (AA) was conjugated to free -NH_2 groups of BSA. In addition to this, AA conjugation to albumin also provides additional hydrophobic domains, which is anticipated to enhance DTX protein

binding affinity. Hence, considering the above mentioned complexities associated with GEM, development of prodrug of GEM could effectively improve the solubility profile, stability, cell uptake and target specificity of GEM. Furthermore, by conjugating AA, the AA-GEM-BSA conjugate was then transformed into NPs, which could also mollify solubility related hurdles of DTX and significant solvent related toxicities including allergic, hypersensitivity and anaphylactic reactions can be resolved. In addition, presence of AA is also anticipated to improve the tumour selectivity (via affinity towards VEGF receptors, overexpressed in tumor angiogenesis) of developed NPs. The simple manufacturing process and use of relatively cost effective excipients offer high level of industrial scalability and applicability.

2 MATERIALS AND METHODS

2.1 Materials

GEM and DTX were provided as gift sample by Fresenius Kabi Oncology Limited, Gurgaon, India. BSA, Anacardic acid (AA), chlorpromazine (CPZ), genistein (GEN) Dimethyl sulfoxide (DMSO), 3-(4,5-dimethylthiazol-2-yl)-2,5-diphenyltetrazolium bromide (MTT), Triton X-100 and ethylene diamine tetra acetic acid (EDTA), N,N'-Carbonyldiimidazole (CDI), 1-Ethyl-3-(3-dimethylaminopropyl)-carbodiimide (EDC), N hydroxyl succinimide (NHS), Minimum essential medium (MEM), Dulbecco's Modified Eagle Medium (DMEM), fetal bovine serum (FBS), antibiotic–antimycotic solution were procured from Sigma Aldrich, USA. Pyridine, and diethyl ether were purchased from Merck. Pyridine were dehydrated over phosphorus pentoxide, respectively, and distilled prior to use. Ultrapure deionized water (LaboStar Ultrapure Water Systems, Germany) was used for all the experiments. All other reagents used were of analytical grade.

2.2 Methods

2.2.1 Synthesis of AA-GEM-BSA Conjugate

The detailed synthesis of conjugate is mentioned in the supporting information.

2.2.2 Preparation of DTX loaded AA-GEM-BSA NPs

AA-GEM-BSA conjugate was further transformed into NPs via high pressure homogenization method with slight modification and extensively optimized using Box-Behnken design via design of expert (Please refer supporting information).[18, 19] Briefly, 100 mg of AA-GEM-BSA conjugate was dissolved in 10 ml of water. To this aqueous solution, 2 ml of 1:1 ratio of ethanol and chloroform, containing 10 mg DTX, was added dropwise (1 ml/min), under a low shear forces (magnetic stirrer) at 1200 rpm for 1 h in order to form a crude emulsion. The above emulsion was subjected to high-pressure homogenization (20000 psi for 10 cycles). Finally, residual chloroform and ethanol were evaporated by rotary evaporation. The aqueous dispersion containing NPs was then centrifuged at 5000 rpm for 5 minutes to pelletized free drug and the supernatant was sterilized by 0.22 µm filter and lyophilized using 5%w/v mannitol. (Please refer supporting information)

2.2.3 Characterization of GEM-BSA NPs

2.2.3.1 Particle size, zeta potential and entrapment efficiency (%EE)

The developed AA-GEM-BSA NPs were evaluated for their mean particle size, PDI, ZP by using Zeta Sizer (Nano ZS, Malvern Instruments, UK). All measurements were carried out after dilution with distilled water.

The percentage of DTX encapsulated (%EE) in AA-GEM-BSA and BSA NPs was determined by using validated HPLC method (please refer supplementary information).[20] Briefly, NPs were centrifuged and the obtained pellet was dissolved in methanol/1 N NaOH mixture (50:50

v/v) and sonicated for 5 min. The solution was centrifuged at 5000 rpm for 5 min and the supernatant was analyzed using the following formula:

$$\%\ \text{Entrapment efficiency} = \frac{\text{Amount of DTX in NPs}}{\text{Amount of DTX used in NPs preparation}} \text{X100}$$

2.2.3.2 Shape and Morphology

The surface morphology of the developed DTX loaded NPs was analyzed by SEM (S-3400N, Hitachi, Japan) by placing a drop of colloidal dispersion of AA-GEM-BSA NPs over a glass coverslip previously adhered to an aluminium stub by a bi-adhesive carbon tape. The drop was air-dried for ~30 min and samples were visualized using SEM at 10 kV.

Further, the three-dimensional (3D) surface morphology of the NPs was also observed via AFM. A Bruker Multimode 8 atomic force microscope with Nanoscope V controller was used for the AFM measurements. Measurements were made in air under ambient conditions using QNM mode. Analysis was obtained using a V-shaped ScanAsyst air probe from Bruker (nominal spring constant 0.4 Nm^{-1}; nominal resonant frequency 70 kHz; nominal length 600 nm). AFM analysis was performed by placing a drop of NPs on the silicon mica and then allowed to dry for ~30 min.

2.2.4 *In vitro* cell culture experiments

2.2.4.1 Cells

MCF-7 and MDA-MB-231 were purchased from ATCC, Manassas, VA, USA and were cultured as per ATCC guidelines.

2.2.4.2 Cell uptake and internalization studies

Qualitative cell uptake and nuclear co-localization study

The cell uptake of AA-GEM-BSA NPs were evaluated as per our previous reports with slight modifications.[20] Briefly, Coumain-6 (C-6) was used as a model dye to evaluate the cellular uptake of drug in different cell types. C-6 loaded AA-GEM-BSA NPs were prepared by following the same preparation of method except taking C-6 instead of DTX. Thereafter, MCF-7 and MDA-MB-231 cells were cultured onto a 6-well plate at a density of 50,000 cells/well and incubated with C-6 loaded AA-GEM-BSA NPs for 4 h. After incubation the cells were washed with Hank's Buffered Salt Solution (HBSS) for three times and fixed with 2.5% glutaraldehyde (Merck, India) and permeabilized with 0.2% Triton X-100. The nuclei of the cells were stained with DAPI (10 µg/ml) (Sigma, USA) and observed under the CLSM (Olympus FV1000).

Quantitative cell uptake study

In case of quantitative cell uptake analysis, DTX loaded NPs and free DTX were incubated with MCF-7 and MDA-MB-231 cells cultured in 6-well plate for different time intervals of 0.5, 1, 2 and 3 h. Furthermore, in order to confirm the targeting ability towards of the developed nanoparticles VEGF receptors overexpressed in MCF7 and MDA-MB-231 cells, uptake study, in presence and absence of AA was also evaluated. After different incubation time intervals, the cells were washed with HBSS three times to remove the extracellular drugs. Further cells were permeabilized with the 0.2% Triton X-100 and internalized drug was extracted with methanol. The cell lysate was collected and centrifuged (Sigma K 300, USA) at 10,000 rpm for 10 min and the supernatant was subjected to HPLC analysis for quantification of internalized drugs.

2.2.4.3 Intracellular trafficking

The intracellular localization of DTX, GEM and DTX loaded AA-GEM-BSA NPs into the lysosomes and endosomes was determined using LysoTracker® (an acidic organelle specific dye; Ex/ Em 577/590 nm). MCF-7 and MDA-MB-231 cells were treated with DTX, GEM and C-6 loaded AA-GEM-BSA NPs at a concentration of 5 µg/ml. After the incubation for 24 h, the media was aspirated and cells were washed thrice with HBSS and further incubated with the media containing LysoTracker® Red (1 µM) for 30 min in the dark. Thereafter, the cells were washed thrice using HBSS and visualized under CLSM under red channel.

2.2.4.4 Annexin-V apoptosis assay

The *in vitro* therapeutic efficacy of DTX loaded AA-GEM-BSA NPs was further assessed as a capability to induce apoptosis in MCF-7 and MDA-MB-231 cells, via standard phosphatidyl serine externalization assay based on Annexin-V binding.[21] Briefly, MCF-7 and MDA-MB-231 cells were seeded at a density of $5x10^4$ cells per well in the 6-well tissue culture plate (Costars, Corning Inc., NY, USA) and kept to attach overnight at 37 ºC and 5% CO_2. The media was then aspirated and cells were treated with media containing samples, equivalent to 10 µg/ml of DTX. After 6 h of incubation, the cells were washed thrice with HBSS and stained with Annexin-V-Cy3.18 conjugate (AnnCy3) and 6-carboxyfluorescein diacetate (6-CFDA) following the manufacturer's protocol (Annexin V-Cy3™ Apoptosis Detection Kit, Sigma, USA).

2.2.4.5 In vitro hemolysis

The toxicity profile of the developed NPs and marketed formulations (Taxotere® and Gemzar®) was evaluated by *in vitro* hemolysis assay as per our previous reports.[22] RBCs were incubated with free drugs (GEM, DTX and combination of GEM and DTX), marketed formulation (Taxotere®, Gemzar® and combination of Taxotere® and Gemzar®) and DTX loaded AA-GEM-

NPs (equivalent to 0.5 mg/ml of DTX), while, Triton X-100 and PBS were used as positive and negative control. After incubation the supernatant was analyzed at 540 nm for hemoglobin (Hb) content and the % hemolysis was determined using following equation:

$$\% \text{ hemolysis} = 100x(Abs-Abs_0)/(Abs_{100}-Abs_0)$$

Where, Abs, Abs_{100} and Abs_0 are the absorbance of the sample, positive and negative control, respectively.

2.2.5 *In vivo* pharmacokinetics

2.2.5.1 Animals and dosing

Female Sprague Dawley (SD) rats of 220-230 g were supplied by the central animal facility (CAF), National Institute of Pharmaceutical Education & Research (NIPER), India following the approval of all the animal protocols by the Institutional Animal Ethics Committee (IAEC). Prior to experiments, the animals were acclimatized under natural light/dark at temperature of 25 ± 2 °C and relative humidity of 50-60% conditions. After 1 week of acclimatization, the animals were randomly distributed into different groups each containing 5 animals. 1^{st}, 2^{nd} and 3^{rd} group of animals received Gemzar®, Taxotere®, and DTX loaded AA-GEM-BSA NPs, respectively. All the samples were parentrally administered via tail vein at a dose equivalent to 2 and 10 mg/kg weight of DTX and GEM, respectively. At predetermined time points, ~0.2 ml blood samples were collected from the tail vein into the centrifuge tubes containing heparin (40 IU/ml of blood). Further, plasma was separated by centrifuging (3000 rcf for 5 min) the blood samples at 4 °C. To 100 µl of plasma, 200 µl of acetonitrile was added to precipitate proteins and again centrifuged at 10,000 rpm for 10 min at 4 °C. The supernatant was then separated and analyzed for drug content by validated HPLC method (please refer supplementary information).

2.2.5.2 Pharmacokinetic data analysis

The pharmacokinetic data was analyzed by one compartmental model, using Kinetica software (Thermo scientific). Required pharmacokinetics parameters like total area under the curve $(AUC)_{0-\infty}$, peak plasma concentration (C_{max}), terminal phase half-life ($t_{1/2}$) and time to reach the maximum plasma concentration (T_{max}) were determined.

2.2.6 Toxicity evaluation

After 7 days of different treatment (Gemzar®, Taxotere®, combination of Gemzar® and Taxotere®, and DTX loaded AA-GEM-BSA NPs), the treated and control animals were sacrificed and blood was collected by cardiac puncture. Thereafter, the plasma was separated and analyzed for various toxicity markers *viz.* alanine transaminase (ALT), aspartate transaminase (AST), blood urea nitrogen (BUN) and creatinine by commercially available diagnostic kits (Accurex Pvt. Ltd., India). From the same group of animals, for the estimation of oxidative stress marker, Malondialdehyde (MDA), liver was isolated and homogenized in 5 volumes of PBS (pH 7.4). In addition, liver, kidney and spleen tissues, excised from each group, were processed as per the routine protocol and further stained with hematoxylin and eosin (H&E) for histopathological evaluations.

2.2.7 *In vivo* haemotoxicity

The effect of Gemzar®, Taxotere®, combination of Gemzar® and Taxotere®, and DTX loaded AA-GEM-BSA NPs treatment on RBCs as compared to control (without treatment) was accessed to analyze haematotoxicity profile in *in-vivo* conditions. Briefly, after 7 days of treatment, RBCs pellet was collected as per the protocol mentioned above. The RBCs pellet was then suspended in 3-fold volume of 0.5% glutaraldehyde in phosphate buffer (pH 7.4) for 60 min

and further washed four times with 10-fold distilled water. Finally, fixed RBCs were imaged under SEM.

2.2.8 *In vivo* bio-distribution

In-vivo bio-distribution of NPs was analyzed by qualitative estimation of fluorescence from C-6 loaded nanoformulation within tumor and organs following i.v. adminstration.[23] Briefly, tumor bearing female Sprague Dawley (SD) rats were divided into three groups, administered with free C-6, C-6 loaded BSA NPs, and C-6 loaded AA-GEM-BSA NPs (equivalent to 0.1 mg/kg of C-6) via tail vein. After the incubation of 24 h, the animals were sacrificed, then the organs (liver, lung, heart, spleen and kidney) and tumor were excised and sectioned. The sections were then visualized by CLSM for the C-6 fluorescense.

2.2.9 *In vivo* antitumor efficacy

DMBA induced breast cancer model was used to evaluate the antitumor efficacy of the developed NPs as per our previous protocol with slight modification.[24, 25] Briefly, DMBA, dissolved in soya bean oil, was orally administered to the rats at 45 mg/kg dose for three consecutive weeks with weekly interval. Once the average tumor volume reached about 100 mm^3, tumor bearing animals were separated and randomly divided into different groups each containing 5 animals. A single dose of Taxotere®, Gemzar®, combination of both Taxotere® and Gemzar® and DTX loaded AA-GEM-BSA NPs (each equivalent to 2 mg/kg of DTX) was administered to the first 4 groups of animals, while, the 5^{th} group (control) received normal saline via I.V. route. The tumor volume was measured on every alternate day with a digital caliper up to 15 days. In addition, survival of the animals was analyzed using the Kaplan−Meier survival plot.

2.2.10 Statistical analysis

All the data are expressed as mean ± standard deviation (SD) and mean ± standard error of mean (SEM) for all *in vitro* and *in vivo* results, respectively. Statistical analysis was performed using Sigma Stat (version 3.5) utilizing one-way ANOVA followed by Tukey−Kramer multiple comparison test. $p<0.05$ was considered as statistically significant difference.

3 RESULTS

3.1 Characterization of AA-GEM-BSA NPs

3.1.1 Shape and Morphology of NPs

The quality attributes (size, PDI, ZP and % drug loading) of developed nanoformulation (AA-GEM-BSA NPs) are shown in **Table 1**. In addition, SEM and AFM analysis confirmed the formation of spherical and smooth surface NPs **(Figure 1).** Moreover, the results were in good correlation with the results obtained from zeta sizer.

3.2 *In vitro* cell culture experiments

3.2.1 Cell uptake

3.2.1.1 Qualitative cell uptake and nuclear co-localization

To support our hypothesis of improved cellular uptake followed by nuclear uptake owing to modification of BSA with AA and GEM, cell uptake and nuclear co-localization assay were performed in MCF-7 **(Figure 2 A and B)** and MDA-MB-231 **(Figure 2 C and D)** cells. As evident from the green florescent panel (b) of **Figure 2,** C-6 loaded AA-GEM-BSA NPs showed significantly higher cellular uptake in both cells lines suggestive of efficient internalization of NPs. Further, the nuclear co-localization of AA-GEM-BSA NPs **(Figure 2 A and C)** was also investigated and compared with non-modified NPs (BSA NPs) **(Figure 2 B and D)**, which demonstrates remarkable fluorescence overlap (**Figure 2,** A and C, panel c) of DAPI (blue

florescence of nucleus staining dye, **Figure 2,** A and C, panel a) and C-6 (green fluorescence of C-6 loaded NPs; **Figure 2,** A and C, panel b) in case of AA-GEM-BSA NPs. In contrast, plain BSA NPs exhibited higher C-6 fluorescence intensity in the cytoplasm (**Figure 2,** B and D).

Efficient nuclear co-localization was also demonstrated via box **(Figure 2,** panel f**)** and line series analysis **(Figure 2,** panel f**)** which validated the overlap of green florescence in case of AA-GEM BSA NPs. Further, remarkably higher nuclear co-localization was evident via Pearson's coefficient between C-6 loaded AA-GEM-BSA NPs and DAPI was found to be 0.91 and 0.83 (**Figure 2,** A and C, panel h), while, the Pearson's coefficient in case of C-6 loaded NPs was found to be 0.43 and 0.44 in MCF-7 and MDA-MB-231, respectively (**Figure 2,** B and D, panel h).

3.2.1.2 Quantitative cell uptake

Time and concentration dependent quantitative cell uptake was also studied, which demonstrated significant enhancement in the cellular uptake of DTX when encapsulated in AA-GEM-BSA NPs as compared to free DTX and DTX loaded BSA NPs (**Figure 2** (II)). Furthermore, pretreatment of MCF-7 and MDA-MB-231 cells with AA could not restrain AA-GEM-BSA NPs from entering the cells, however, a prominent difference in the DTX concentration was noticed.

3.2.2 Intracellular trafficking

Subcellular fate of DTX, GEM, combination of DTX and DTX loaded BSA NPs and DTX loaded AA-GEM-BSA NPs was evaluated by using LysoTracker® Red dye. **Figure 3** shows the comparative formation of lysosomes following the treatment of cells with DTX , GEM, combination of DTX and GEM, DTX loaded BSA NPs and DTX loaded AA-GEM-BSA NPs for 24 h. Cells incubated with DTX loaded AA-GEM-BSA NPs and DTX loaded BSA NPs exhibited significantly higher red fluorescence intensity (LysoTracker® Red dye, **Figure 3,** panel

a) as compared to the cells treated with free drugs and their combination. Furthermore, to validate the overlapping of LysoTracker® fluorescence with the differential interface contrast images of cells (**Figure 3,** panel c), vertical (**Figure 3,** panel d) and horizontal (**Figure 3,** panel e) line series analysis was performed, which demonstrated significant overlapping of LysoTracker® red fluorescence signals with the vibrations of white lines (corresponding with cells signals), revealing significantly higher lysosome formation in case of NPs treatment.

3.2.3 Annexin-V apoptosis assay

Significantly higher levels of apoptosis index was observed in case of DTX loaded AA-GEM–BSA NPs in comparison with individual drugs and their combination (DTX+GEM) in both MCF-7 and MDA-MB-231 cell lines (**Figure 4).** The apoptotic index in case of DTX, GEM and their combination (DTX+GEM) was found to be 0.54, 0.42 and 0.72, respectively in MCF-7 cell lines. This went even higher up to 0.67 and 0.98 in case of blank AA-GEM-ALB NPs and DTX loaded AA-GEM-BSA NPs, respectively. Similar trend was observed in MDA-MB-231 cell lines.

3.2.4 *In vitro* hemolysis

Complete hemolysis was noticed when incubated with Triton X 100 (positive control), while, no hemolysis was found in case of PBS, pH 7.4 (negative control). Incubation of RBCs with free DTX, free GEM, combination of free GEM and DTX, Taxotere®, Gemzar® and combination of marketed formulations demonstrated almost 21.07, 20.83, 37.18, 25.75, 21.52 and 41.06 % hemolysis, respectively. In contrast, DTX loaded NPs demonstrated no sign of hemolysis and found to be comparable with negative control (**Figure 7** F).

3.3 *In vivo* study

3.3.1 Pharmacokinetics

Different pharmacokinetic parameters of DTX following *i.v.* administration of Taxotere® and DTX loaded AA-GEM-BSA NPs is summarized in **Table 2**. The $AUC_{(0-\infty)}$ and $T_{1/2}$ value of DTX was found to be 6.12 and 6.28-fold higher, respectively, in case of DTX loaded AA-GEM-BSA NPs in comparison with Taxotere® (**Figure 5**). AA-GEM-BSA NPs demonstrated 3.72 and 8.90-fold higher $AUC_{(0-\infty)}$ and $T_{1/2}$ values of GEM as compared to Gemzar®.

3.3.2 Toxicity evaluation

Figure 6 (I) represents the different levels of biochemical parameters following the treatment of marketed formulations, their combination and DTX loaded AA-GEM-BSA NPs. No significant difference was observed in biomarkers levels between the control and the DTX loaded AA-GEM-BSA NPs treated groups. A significant increase in AST, ALT and MDA levels was noticed in Taxotere® and Gemzar® treated animals as compared to control animals.

In line with the hepatotoxic results, BUN and creatinine levels were found to be significantly higher when the animals were treated with Taxotere®, Gemzar®, their combination (Taxotere®, Gemzar®) as compared with control.

The *in vivo* toxicity was further estimated by histopathological examinations of kidney, liver and spleen. Histological sections of animals treated with Taxotere®, Gemzar® and their combination exhibited pronounced level of toxicity as compared to the control animals (**Figure 6** (II)). Interestingly, animals treated with DTX loaded AA-GEM-BSA NPs demonstrated normal parenchymal cell physiology without having sign of inflammation, lesions and necrosis.

3.3.3 *In vivo* hemolysis

The hemolytic effect was evaluated via isolating RBCs from the animals, treated with different sample and observed by SEM for any alteration in morphology. As evident from the **Figure 7**, Taxotere®, Gemzar® and their combination exhibited severe alteration and surface deformities in shape and morphology of RBCs, indicative of hemolytic toxicity. In line with the *in vitro* hemolysis results, no noticeable change in morphology of RBCs was observed in the animals treated with DTX loaded AA-GEM-BSA NPs.

3.3.4 *In vivo* bio-distribution

Figure 8 (I) and (II) depicts bio-distribution of C-6 fluorescence on i.v. administration of free C-6 and C-6 loaded NPs after 24 h, in various organs and tumor. The organ distribution profile of C-6 loaded NPs were significantly differed as compared to free C-6, which suggests higher green fluorescence in tumor sections of animals administered with C-6 loaded AA-GEM-BSA NPs and C-6 loaded BSA NPs. In contrast, higher fluorescence of free C-6 was observed in kidney, liver, heart and spleen as compared with C-6 loaded NPs, while, insignificant difference in fluorescence intensity was found in lungs tissue.

3.3.5 *In vivo* antitumor efficacy

Figure 8 (III) shows the antitumor activity and tumor burden of marketed formulation Gemzar®, Taxotere®, their combination and DTX loaded AA-GEM-BSA NPs following the *i.v.* administration. DTX loaded AA-GEM-BSA NPs treated animals demonstrated significant suppression of tumor growth ($p < 0.001$) as compared to control group. After 15 days of treatment, tumor size was found to be 35.72% in case of DTX loaded AA-GEM-BSA NPs as compared to untreated group (tumor size of 158.29%).

4 DISCUSSION

In the preset report, we have hypothesized a system for the combination therapy of GEM and DTX for synergistic efficacy and reduced toxicity. In order to overcome the challenges of GEM (high water solubility ~83 mg/ml and very short plasma half-life ~45 min), conjugate of AA-GEM-BSA was synthesized to overcome the high solubility issues by having proper hydrophilic-lypophilic balance. In addition, AA was supposed to provide functionality by targeting VEGF receptors to improve the tumor selectivity of NPs and transport of the drugs from cell membrane to nuclear (site of action of GEM) and perinuclear region (site of action of DTX) through ligand-receptor interaction leading to enhanced tumor load of the drugs and therapeutic efficacy. The BSA conjugate of the GEM was synthesized via conjugating 4-(N) position of GEM with –COOH groups of the BSA through a hydrolysable amide linkage, to protect its deamination from cytidine deaminase (CDA), which may result in increase of drug stability, plasma half-life and also minimizes non-specific drug toxicity on normal tissue by preventing *in vivo* random distribution of the drug via enhanced permeability and retention (EPR) effect.[26]

To prove our hypothesis, AA-GEM-BSA conjugate was synthesized by using EDC/NHS carbodiimide chemistry and characterized via ^{1}H NMR and FTIR. The degree of modification, for AA, was evaluated via TNBS method, which was found to be 13.35%, i.e., 24.4 µM AA molecules were conjugated with the equimolar concentration of amine groups in the BSA. The conjugation of GEM with the carboxyl group was evaluated via calorimetric titration method, which demonstrated 24.6 µM GEM were conjugated with the BSA. Ratio of AA, GEM and BSA was found to be 24.4µM: 24.6 µM: 3.0303µM (~8 moles of AA and GEM conjugated with 1 mole of BSA). Increase in BSA molecular weight owing to conjugation of AA and GEM was confirmed by MALDI-TOF, which demonstrates ~7.9 and ~8.5 moles of AA and GEM conjugated to BSA. Shift in gel electrophoresis bands further confirmed the higher molecular

weight of AA-GEM-BSA conjugate. The elemental analysis showed increase in the nitrogen content in case of GEM-BSA conjugate due to the presence of additional 3 nitrogen atoms (1 in $–NH_2$ group and 2 in pyrimidine ring) of GEM. In case of AA-GEM conjugate only percent content of carbon was increased and could be attributed to the presence of long carbon chain in AA. Slight decrease in the sulfur content could be explained by absence of sulfur in both AA and GEM and increased molecular weight of the final conjugate.

Conjugation of AA and GEM resulted in alteration of native conformational structure of BSA, evaluated via measuring intrinsic fluorescence quenching, CD and Raman spectroscopy. BSA displays fluorescence due to the presence of tryptophan moieties at position 134 and 212 in subdomain IB and IIA, respectively. Upon conjugation of both GEM and AA, the fluorescence of BSA was found to be significantly quenched and could be ascribed to the conformational alteration surrounding the tryptophan moieties.[27] In line with the fluorescence quenching, CD spectra overlay also demonstrated alteration in the 3D structure of GEM-BSA, AA-BSA and AA-GEM BSA conjugate as compared with native BSA. Furthermore, structural changes in amide I band (α-helical conformation from peptide C = O stretching vibration, at ~1650 cm^{-1}), amide III band (C-N bond stretching and in-plane N-H bond bending) and skeletal vibration regions was evaluated via Raman spectroscopy.[28] **Table S 7** demonstrates increase (I_{1246}/I_{1337} ratio; from 0.697 to 1.158) and decrease (I_{934}/I_{1003} ratio; from 0.678 to 0.366) in intensity of BSA on conjugation of AA and GEM, which might be due to the increase in random coil and loss of secondary structural content in BSA, respectively.[29] This conformational change in AA-GEM-BSA conjugate is expected for higher cellular uptake of modified NPs as compared to native BSA NPs *via* gp18 and gp30 receptors (over expressed in cancer cells, responsible for uptake of

conformationally altered albumin), in addition to the SPARC (Secreted Protein, Acidic and Rich in Cysteine), mediated uptake of albumin.[30, 31]

The effect of AA and GEM conjugation on the thermal property of BSA was tested by TGA analysis, which demonstrated two major phases of degradation. The initial degradation phase was observed between room temperature to the ~105 °C, this loss of weight could be due to the loss of water molecules in the samples.[32] On further increasing the temperature, the conjugates and native BSA demonstrates second phase of weight loss, which exhibits 10.46, 7.10 and 13.70% higher decomposition in case of GEM-BSA conjugate, AA-BSA conjugate and AA-GEM-BSA conjugate, respectively, as compared to BSA at 300 °C. Furthermore, thermal property of the conjugates was also evaluated via DSC analysis, which depicts presence of no endothermic peaks at ~273°C, corresponding to melting point of GEM, signifying loss of crystalline structure on conjugation with BSA.

The wettability of the synthesized conjugates was measured by contact angle analysis. It is evident from **Figure S 4 (C) and (D)**, on conjugating GEM with BSA, the hydrophilicity of the system was increased resulting in stronger affinity towards the water droplet indicating significantly higher wettability. In contrast, as compared to BSA, owing to its lipophilic nature of AA, AA-BSA conjugate demonstrated higher contact angle with water droplet indicating lower affinity towards water droplet. Interestingly, on conjugation of both AA and GEM the amphiphilic nature of the system was found to be comparative to BSA and could be attributed to the hydrophilic-lipophilic balance provided by both AA and GEM.

The synthesized AA-GEM-BSA conjugate was then utilized for the preparation of NPs by high pressure homogenization and extensively optimized via Box-Behnken design. The critical quality attributes such as size and PDI of developed NPs were found to be 139±7 nm, 0.13±0.04

and 163±8 nm, 0.13±0.09 in case of BSA NPs and AA-GEM-BSA NPs, respectively. Interestingly, BSA NPs exhibited ZP -35±2 mV, while in case of AA-GEM-BSA NPs the ZP was found to be -27±1 mV. This depreciation in ZP could be attributed to reduction in amino groups following the conjugation with AA.

To improve the storage stability of the formulations, NPs were freeze dried by using cryoprotectant. Among various cryoprotectants (**Table S7**), mannitol was employed as the optimized one owing to formation of stable network around the NPs leading to minimal changes in the critical quality attributes of NPs. The powder X-ray diffraction (PXRD) spectra of developed NPs demonstrate absence of characteristics peaks of DTX and GEM, suggesting existence of drugs in the amorphous form rather than crystalline form. Furthermore, the stability of the developed NPs at accelerated storage conditions were also evaluated, which demonstrates excellent storage stability at accelerated storage condition (**Table S 11**).

In vitro release study demonstrated significant retardation of DTX release from AA-GEM-BSA NPs as compared to BSA NPs. This depreciation could be due to the conjugation of AA and GEM, which acts as a barrier for the release of drug from the albumin matrix as compared to BSA NPs. Further, the release kinetics of NPs was also evaluated which demonstrated Higuchi kinetics of drug release, depicting involvement of initial diffusion followed by erosion, disintegration from the matrix of NPs.[33] **Figure S 8** demonstrated higher release of GEM from NPs at pH 5.5 as compared to pH 7.4 in the presence of protease. In plasma stability studies, GEM showed rapid degradation into its inactive metabolite dFdU (~64%), while, this was ~16% in case of NPs following the 24 h incubation in plasma. The sustained release and enhanced stability against enzymatic degradation could be attributed to the stability of amide bond.[34]

Furthermore, higher drug release at pH 5.5 can be a useful property to get maximum release of GEM at tumor environment.

To support our hypothesis of improved cellular uptake followed by nuclear uptake owing to modification of BSA with AA and GEM, cell uptake and nuclear co-localization assay were performed in MCF-7 and MDA-MB-231 cells. Random distribution of green fluorescence throughout the cell (nuclear and perinuclear region) was observed in case of C-6 loaded AA-GEM-BSA NPs which could be attributed to the modification of BSA with AA. In contrast, BSA NPs demonstrated negligible C-6 fluorescence in the nuclear portion of cells. Furthermore, quantitative cell uptake study demonstrated higher cellular uptake of DTX loaded AA-GEM-BSA NPs as compared to free drug and DTX loaded BSA NPs. This appreciation in the cell permeability in case of NPs could be attributed to the gp 18 and gp 30 transporters, overexpressed in breast cancer cell lines.[35] Furthermore, by conjugating with AA, BSA NPs can be directed to the desired site of drug action (nuclear and perinuclear region), owing to higher affinity of AA towards ER-selective Nuclear Receptor Alternative Site Modulators (NRAMs) and zinc fingers of the DNA Binding Domain (estrogen-responsive elements; resulting from high metal-chelating property of AA).[36, 37] The transport of hydrophobic moieties such as AA is also reported to alter the conformation and permeability of the nuclear pore complex leading to increased nuclear trafficking.[38]

The cell uptake study revealed efficient internalization of NPs, which might be ascribed to different mechanism of internalization. Thus to further explore the Intracellular trafficking or fate of NPs in MCF-7 and MDA-MB-231 cell lines, LysoTracker® red dye was used. As evident from **Figure 3**, negligible fluorescence of LysoTracker® red dye was seen in case of control cells (without treatment) and cells incubated with DTX, GEM and combination of DTX and

GEM. In contrast, cells treated with NPs exhibits significantly higher fluorescence, demonstrating radical increase in the lysosome formation within the MCF-7 and MDA-MB-231, indicative of endocytic uptake of NPs through endo-lysosomes pathway.

The transportation of DTX and GEM across the cell membrane requires specific transporters such as hNTs (human equilibrative nucleoside transporters, hENTs and human concentrative nucleoside transporters, hCNTs) and OATPs (organic anion transporting polypeptide) transporters, respectively, which acts as a limiting factor for their therapeutic efficacy. Thus, to explore the reliance on hNTs and OATPs, MCF-7 and MDA-MB-231 cells were pre-incubated with dipyridamole (hNTs and OATP1B3 inhibitor) followed by treatment with NPs and free drugs.[39, 40] **Table S24** depicts, dipyridamole mediated transporters inhibition, which significantly increased the IC_{50} value of free drugs. In contrast, insignificant change in IC_{50} was observed in case of NPs in both MCF-7 and MDA-MB-231 cells. The insignificant change in IC_{50} or resistance towards drug cytotoxicity suggested existence of additional endocytic cell uptake or internalization mechanism, bypassing hNTs and OATPs mediated uptake in case of DTX loaded NPs. To further explore the plausible mechanism of NPs uptake, the cells were pre incubated with different inhibitors (GNT; caveolae uptake inhibitor and CPZ; clathrin uptake inhibitor). As evident from **Table S24**, increase in IC_{50} values was observed in case of NPs treatment, pre-incubated with GNT and CPZ. However, increase in IC_{50} or resistance, when the cells were pre-incubated with GNT, was not as prominent as compared to CPZ, indicating contribution of both clathrin and caveolae dependent cell uptake mechanism, while clathrin mediated uptake as primary mechanism. The results were in line with the cell uptake study revealing clathrin and caveolae mediated endocytic pathway of NPs.[41]

The cell cytotoxicity experiments revealed significantly higher concentration and time dependent cell cytotoxicity of NPs as compared to that of GEM, DTX and combination of both GEM and DTX. The increased cytotoxicity could be ascribed to enhanced cellular uptake of NPs via clathrin dependent endocytosis and higher stability of GEM against CDA mediated degradation. The cell cytotoxicity was further corroborated by *in vitro* DNA damage and Annexin-V apoptosis assay. DNA damage is the primary mechanism of cytotoxicity in case of GEM, while, it is also reported that microtubule-targeting agents, such as DTX, also exhibits DNA damage by disrupting intracellular trafficking of DNA repair proteins.[42] DTX loaded AA-GEM-BSA NPs exhibited significantly higher DNA damage as compared to the combination of GEM and DTX, which could be attributed to the enhanced availability of DTX and GEM in case of NPs. The results depicted, cytotoxicity potential of both GEM and DTX was preserved on conjugation and encapsulation within the NPs, respectively, and is efficiently transported to the nuclear and perinuclear fraction of the MCF-7 and MDA-MB-231 cells. Furthermore, Annexin-V apoptosis assay revealed higher apoptotic index in MCF-7 and MDA-MB-231 cell lines, when incubated with NPs, in comparison with individual drugs and their combination.

The Hemolytic toxicity of marketed formulations (Taxotere®, Gemzar®), their combination and DTX loaded NPs demonstrated severe Hemolytic toxicity of the marketed formulations and their combination while insignificant changes in NPs as compared to control (RBCs treated with PBS) **Figure 7** F. This relatively lower hemolysis, observed in case of NPs, could be ascribed to the absence of Tween 80 and ethanol (solvent system of Taxotere®) and reduced exposure of individual drug.

Taxotere® and DTX loaded NPs were evaluated for their pharmacokinetics profiles after *i.v.* administration. AA-GEM-BSA NPs demonstrated improved pharmacokinetic profile showing

significant amelioration in the DTX and GEM levels with 6.12 and 3.27-fold and 6.28 and 8.9-fold higher AUC and $T_{1/2}$ values as compared to Taxotere® and Gemzar®, respectively. This increment of AUC and $T_{1/2}$ values could be due to increase in circulation time of the drug owing to sustained release from NPs and enhancement in circulation half-time owing to longer albumin blood half-life (achieved through protein recycling via different physiological mechanisms). The increase in blood residence time of drugs could be by virtue of the enhanced molecular weight and encapsulation within the BSA NPs, leading to reduced susceptibility towards renal clearance or filtration.[43]

Taxotere® and Gemzar® are primarily excreted via hepatobiliary and renal clearance, respectively, thus, demonstrates significant hepato and renal toxicity. **Figure 6** depicts significantly higher levels of AST and ALT in group of animals treated with Gemzar®, Taxotere® and their combination, while, DTX loaded AA-GEM-BSA NPs demonstrated insignificant difference in AST and ALT levels in comparison with the control animals. In addition, the MDA levels further validated the absence of toxicity or oxidative stress in group of animals treated with NPs. Furthermore, various nephrotoxicity markers such as BUN and creatinine levels were also measured, which demonstrated significantly higher levels in case of marketed formulations as compared to control and NPs treated animals. Relatively lower toxicity profile in case of NPs treatment could be attributed to absence of vehicle, long circulation time and sustained release of drugs. The histopathological evaluation of liver, spleen and kidney was performed to analyze solvent and drug induced toxicity. As evident from the **Figure 6** (III), no indication of toxicity was found in case of treatment with NPs, while, severe lesions, loss of cellular integrity and inflammation was observed, when treated with Gemzar®, Taxotere® and their combination. *In vivo* real time Hemolytic activity after *i.v.* administration of formulations

was evaluated for qualitative Hemolytic toxicity via SEM. RBCs isolated from the animals treated with marketed formulations, demonstrated significant alteration in surface morphology with pronounced surface roughness/ deformity and even change in physiology while no visual change could be detected in case of RBCs from NPs treated groups as compared to RBCs taken out from control animals.

The organ distribution of C-6 loaded NPs were assessed by in-vivo imaging to evaluate the potential of developed nanoformulations to effectively target drugs into the tumor environment bypassing non targeted organs i.e., heart, liver, kidney, lung, spleen, etc. After 24 h of administration significantly higher fluorescence intensity was observed in tumor, while, lower fluorescence was found in non-targeted organs when the animals were administered with C-6 loaded AA-GEM-BSA NPs. Interestingly, the fluorescence intensity of C-6 loaded AA-GEM-BSA NPs was found to be even higher compared with plain C-6 loaded BSA NPs in tumor. This observation could be attributed to higher affinity of AA towards VEGF receptors, overexpressed in tumor angiogenesis, confirming tumor targeting potential of developed AA-GEM modified BSA NPs.

Further, the *in vivo* pharmacodynamic efficacy of developed NPs was tested in DMBA induced breast cancer tumor model. Treatment with DTX loaded AA-GEM-BSA NPs demonstrated significant reduction in the tumor burden in comparison with marketed formulations (Gemzar®, Taxotere®) and their combination. The higher C-6 fluorescence intensity in tumor sections and increased therapeutic efficacy in case of NPs could be attributed to sustained pharmacokinetic pattern responsible for longer availability of DTX and GEM in the blood compartment and by the virtue of enhanced permeation and retention (EPR). According to reports, the endothelial transportation of native BSA NPs from blood vessels to tumor environment takes place via

SPARC (Secreted Protein, Acidic and Rich in Cysteine) and caveolae (mediated by gp60 transporters) mechanism. Enhanced efficacy and tumor accumulation in case of developed AA-GEM BSA NPs could be attributed to higher uptake by both clathrin (mediated by AA affinity towards VEGF receptors) in addition to the caveolae mediated uptake.[44, 45] Furthermore, pronounced increase in SPARC and VEGF expression is reported to be upregulated in multiple tumors, will ensure selective distribution of drug loaded NPs in the tumor vicinity, which, in turn, is expected to enhance the therapeutic efficacy of the loaded drug with reduced drug induced toxicity. Kaplan Meier survival curve (**Figure 8** (D)) showed enhanced survival time of tumor bearing rats in NPs treated groups as compared to DMBA control and other groups suggestive of lower toxicity and higher safety of the developed combinatory strategy.

5 CONCLUSION

In the present report, a combinatory strategy was hypothesized to deliver GEM and DTX in a single smart delivery vehicle. AA functionalized DTX loaded NPs demonstrated sustained release, higher cellular uptake in the perinuclear and nuclear region (nuclear co-localization) via hNTs and OATP1B3 independent clathrin mediated internalization, significant reduction in IC_{50} value and higher apoptotic index. Interestingly, developed NPs showed significant improvement in pharmacokinetic and pharmacodynamics by simultaneously alleviating the toxicities associated with marketed formulations. Fruitful outcomes of the present strategy offer an additional research horizon of drug macromolecule conjugates to overcome the limitations of hydrophobic and hydrophilic drugs molecules and has the promising potential to act as a platform technology for the delivery of potent but difficult to deliver drugs with limited clinical efficacy.

ACKNOWLEDGEMENT

The authors are thankful to the Director NIPER, James Graham Brown Cancer Center (University of Louisville, KY, USA) and Strathclyde Institute of Pharmacy & Biomedical Sciences (University of Strathclyde, Glasgow, U.K.) for necessary infrastructure and facilities. Varun Kushwah is also grateful to the Council of Scientific and Industrial Research (CSIR), GOI, New Delhi (Grant ID 09/727(0107)/2013-EMR-I), United States-India Educational Foundation, New Delhi (Grant ID PS00218456) and Commonwealth commission in the UK (Grant ID INCN-2015-29) for providing research funding and fellowships. He was the 2016-17 Fulbright-Nehru Doctoral and 2015-16 Commonwealth Split-site PhD research fellow at University of Louisville, Louisville, KY and University of Strathclyde, Glasgow, U.K., respectively.

Conflict of Interest and Disclosure

The authors report no financial interest that might pose a potential, perceived, or real conflict of interest.

REFERENCE

[1] N.K. Swarnakar, K. Thanki, S. Jain, Enhanced antitumor efficacy and counterfeited cardiotoxicity of combinatorial oral therapy using Doxorubicin-and Coenzyme Q10-liquid crystalline nanoparticles in comparison with intravenous Adriamycin, Nanomedicine: Nanotechnology, Biology and Medicine 10(6) (2014) 1231-1241.

[2] M. Das, R. Jain, A.K. Agrawal, K. Thanki, S. Jain, Macromolecular bipill of gemcitabine and methotrexate facilitates tumor-specific dual drug therapy with higher benefit-to-risk ratio, Bioconjugate chemistry 25(3) (2014) 501-509.

[3] R.G. Maki, J.K. Wathen, S.R. Patel, D.A. Priebat, S.H. Okuno, B. Samuels, M. Fanucchi, D.C. Harmon, S.M. Schuetze, D. Reinke, Randomized phase II study of gemcitabine and docetaxel compared with gemcitabine alone in patients with metastatic soft tissue sarcomas: results of sarcoma alliance for research through collaboration study 002, Journal of Clinical Oncology 25(19) (2007) 2755-2763.

[4] M.L. Hensley, J.A. Blessing, R. Mannel, P.G. Rose, Fixed-dose rate gemcitabine plus docetaxel as first-line therapy for metastatic uterine leiomyosarcoma: a Gynecologic Oncology Group phase II trial, Gynecologic oncology 109(3) (2008) 329-334.

[5] D. Mavroudis, N. Malamos, A. Alexopoulos, C. Kourousis, S. Agelaki, E. Sarra, A. Potamianou, C. Kosmas, G. Rigatos, T. Giannakakis, Salvage chemotherapy in anthracycline-pretreated metastatic breast cancer patients with docetaxel and gemcitabine: a multicenter phase II trial, Annals of oncology 10(2) (1999) 211-215.

[6] W. Plunkett, P. Huang, Y.-Z. Xu, V. Heinemann, R. Grunewald, V. Gandhi, Gemcitabine: metabolism, mechanisms of action, and self-potentiation, Seminars in oncology, 1995, pp. 3-10.

[7] F. Lavelle, M. Bissery, C. Combeau, J. Riou, P. Vrignaud, S. Andre, Preclinical evaluation of docetaxel (Taxotere), Seminars in oncology, 1995, pp. 3-16.

[8] A.M. Storniolo, S. Allerheiligen, H.L. Pearce, Preclinical, pharmacologic, and phase I studies of gemcitabine, Seminars in oncology, 1997, pp. S7-2-S7-7.

[9] S. Jain, G. Spandana, A.K. Agrawal, V. Kushwah, K. Thanki, Enhanced antitumor efficacy and reduced toxicity of docetaxel loaded estradiol functionalized stealth polymeric nanoparticles, Molecular pharmaceutics 12(11) (2015) 3871-3884.

[10] F.K. Engels, R.A. Mathot, J. Verweij, Alternative drug formulations of docetaxel: a review, Anti-cancer drugs 18(2) (2007) 95-103.

[11] N.V. Koshkina, E.S. Kleinerman, Aerosol gemcitabine inhibits the growth of primary osteosarcoma and osteosarcoma lung metastases, International journal of cancer 116(3) (2005) 458-463.

[12] M.N. Khalid, P. Simard, D. Hoarau, A. Dragomir, J.-C. Leroux, Long circulating poly (ethylene glycol)-decorated lipid nanocapsules deliver docetaxel to solid tumors, Pharmaceutical research 23(4) (2006) 752-758.

[13] W. Tao, X. Zeng, J. Wu, X. Zhu, X. Yu, X. Zhang, J. Zhang, G. Liu, L. Mei, Polydopamine-based surface modification of novel nanoparticle-aptamer bioconjugates for in vivo breast cancer targeting and enhanced therapeutic effects, Theranostics 6(4) (2016) 470.

[14] W. Tao, X. Zeng, T. Liu, Z. Wang, Q. Xiong, C. Ouyang, L. Huang, L. Mei, Docetaxel-loaded nanoparticles based on star-shaped mannitol-core PLGA-TPGS diblock copolymer for breast cancer therapy, Acta biomaterialia 9(11) (2013) 8910-8920.

[15] L. Sun, D.-S. Zhou, P. Zhang, Q.-H. Li, P. Liu, Gemcitabine and γ-cyclodextrin/docetaxel inclusion complex-loaded liposome for highly effective combinational therapy of osteosarcoma, International journal of pharmaceutics 478(1) (2015) 308-317.
[16] Y. Fan, Q. Wang, G. Lin, Y. Shi, Z. Gu, T. Ding, Combination of using prodrug-modified cationic liposome nanocomplexes and a potentiating strategy via targeted co-delivery of gemcitabine and docetaxel for CD44-overexpressed triple negative breast cancer therapy, Acta biomaterialia 62 (2017) 257-272.
[17] V. Khare, S. Kour, N. Alam, R.D. Dubey, A. Saneja, M. Koul, A.P. Gupta, D. Singh, S.K. Singh, A.K. Saxena, Synthesis, characterization and mechanistic-insight into the anti-proliferative potential of PLGA-gemcitabine conjugate, International journal of pharmaceutics 470(1) (2014) 51-62.
[18] T.H. Kim, H.H. Jiang, Y.S. Youn, C.W. Park, K.K. Tak, S. Lee, H. Kim, S. Jon, X. Chen, K.C. Lee, Preparation and characterization of water-soluble albumin-bound curcumin nanoparticles with improved antitumor activity, International journal of pharmaceutics 403(1) (2011) 285-291.
[19] N.P. Desai, C. Tao, A. Yang, L. Louie, Z. Yao, P. Soon-Shiong, S. Magdassi, Protein stabilized pharmacologically active agents, methods for the preparation thereof and methods for the use thereof, Google Patents, 2004.
[20] B. Hoang, M.J. Ernsting, A. Roy, M. Murakami, E. Undzys, S.-D. Li, Docetaxel-carboxymethylcellulose nanoparticles target cells via a SPARC and albumin dependent mechanism, Biomaterials 59 (2015) 66-76.
[21] C.P. Dora, F. Trotta, V. Kushwah, N. Devasari, C. Singh, S. Suresh, S. Jain, Potential of erlotinib cyclodextrin nanosponge complex to enhance solubility, dissolution rate, in vitro cytotoxicity and oral bioavailability, Carbohydrate polymers 137 (2016) 339-349.
[22] S. Jain, P.U. Valvi, N.K. Swarnakar, K. Thanki, Gelatin coated hybrid lipid nanoparticles for oral delivery of amphotericin B, Molecular pharmaceutics 9(9) (2012) 2542-2553.
[23] X. Li, F. Qin, L. Yang, L. Mo, L. Li, L. Hou, Sulfatide-containing lipid perfluorooctylbromide nanoparticles as paclitaxel vehicles targeting breast carcinoma, International journal of nanomedicine 9 (2014) 3971.
[24] S. Jain, T. Garg, V. Kushwah, K. Thanki, A.K. Agrawal, C.P. Dora, α-Tocopherol as functional excipient for resveratrol and coenzyme Q10-loaded SNEDDS for improved bioavailability and prophylaxis of breast cancer, Journal of drug targeting 25(6) (2017) 554-565.
[25] S. Tripathi, V. Kushwah, K. Thanki, S. Jain, Triple antioxidant SNEDDS formulation with enhanced oral bioavailability: Implication of chemoprevention of breast cancer, Nanomedicine: Nanotechnology, Biology and Medicine 12(6) (2016) 1431-1443.
[26] D. Chitkara, A. Mittal, S.W. Behrman, N. Kumar, R.I. Mahato, Self-assembling, amphiphilic polymer–gemcitabine conjugate shows enhanced antitumor efficacy against human pancreatic adenocarcinoma, Bioconjugate chemistry 24(7) (2013) 1161-1173.
[27] M. Ghali, Static quenching of bovine serum albumin conjugated with small size CdS nanocrystalline quantum dots, Journal of Luminescence 130(7) (2010) 1254-1257.
[28] B.A. Bolton, J.R. Scherer, Raman spectra and water absorption of bovine serum albumin, The Journal of Physical Chemistry 93(22) (1989) 7635-7640.
[29] V. Lin, J. Koenig, Raman studies of bovine serum albumin, Biopolymers 15(1) (1976) 203-218.

[30] J. Schnitzer, J. Bravo, High affinity binding, endocytosis, and degradation of conformationally modified albumins. Potential role of gp30 and gp18 as novel scavenger receptors, Journal of Biological Chemistry 268(10) (1993) 7562-7570.
[31] J. Schnitzer, A. Sung, R. Horvat, J. Bravo, Preferential interaction of albumin-binding proteins, gp30 and gp18, with conformationally modified albumins. Presence in many cells and tissues with a possible role in catabolism, Journal of Biological Chemistry 267(34) (1992) 24544-24553.
[32] M.W. Ahmad, C.R. Kim, J.S. Baeck, Y. Chang, T.J. Kim, J.E. Bae, K.S. Chae, G.H. Lee, Bovine serum albumin (BSA) and cleaved-BSA conjugated ultrasmall Gd 2 O 3 nanoparticles: Synthesis, characterization, and application to MRI contrast agents, Colloids and Surfaces A: Physicochemical and Engineering Aspects 450 (2014) 67-75.
[33] T. Higuchi, Mechanism of sustained-action medication. Theoretical analysis of rate of release of solid drugs dispersed in solid matrices, Journal of pharmaceutical sciences 52(12) (1963) 1145-1149.
[34] E. Moysan, G. Bastiat, J.-P. Benoit, Gemcitabine versus modified gemcitabine: a review of several promising chemical modifications, Molecular pharmaceutics 10(2) (2012) 430-444.
[35] A.M. Merlot, D.S. Kalinowski, D.R. Richardson, Unraveling the mysteries of serum albumin—more than just a serum protein, Frontiers in physiology 5 (2014) 299.
[36] L. Caboni, D.G. Lloyd, Beyond the Ligand-Binding Pocket: Targeting Alternate Sites in Nuclear Receptors, Medicinal research reviews 33(5) (2013) 1081-1118.
[37] D.J. Schultz, N.S. Wickramasinghe, M.M. Ivanova, S.M. Isaacs, S.M. Dougherty, Y. Imbert-Fernandez, A.R. Cunningham, C. Chen, C.M. Klinge, Anacardic acid inhibits estrogen receptor α–DNA binding and reduces target gene transcription and breast cancer cell proliferation, Molecular cancer therapeutics 9(3) (2010) 594-605.
[38] B. Naim, D. Zbaida, S. Dagan, R. Kapon, Z. Reich, Cargo surface hydrophobicity is sufficient to overcome the nuclear pore complex selectivity barrier, The EMBO Journal 28(18) (2009) 2697-2705.
[39] M. Karlgren, A. Vildhede, U. Norinder, J.R. Wisniewski, E. Kimoto, Y. Lai, U. Haglund, P. Artursson, Classification of inhibitors of hepatic organic anion transporting polypeptides (OATPs): influence of protein expression on drug–drug interactions, Journal of medicinal chemistry 55(10) (2012) 4740-4763.
[40] J.R. Mackey, R.S. Mani, M. Selner, D. Mowles, J.D. Young, J.A. Belt, C.R. Crawford, C.E. Cass, Functional nucleoside transporters are required for gemcitabine influx and manifestation of toxicity in cancer cell lines, Cancer research 58(19) (1998) 4349-4357.
[41] K.R. Chaudhari, A. Kumar, V.K.M. Khandelwal, M. Ukawala, A.S. Manjappa, A.K. Mishra, J. Monkkonen, R.S.R. Murthy, Bone metastasis targeting: a novel approach to reach bone using Zoledronate anchored PLGA nanoparticle as carrier system loaded with Docetaxel, Journal of controlled release 158(3) (2012) 470-478.
[42] M.S. Poruchynsky, E. Komlodi-Pasztor, S. Trostel, J. Wilkerson, M. Regairaz, Y. Pommier, X. Zhang, T.K. Maity, R. Robey, M. Burotto, Microtubule-targeting agents augment the toxicity of DNA-damaging agents by disrupting intracellular trafficking of DNA repair proteins, Proceedings of the National Academy of Sciences 112(5) (2015) 1571-1576.
[43] R.E. Kontermann, Strategies for extended serum half-life of protein therapeutics, Current Opinion in Biotechnology 22(6) (2011) 868-876.
[44] I. Neil, Nab technology: a drug delivery platform utilizing endothelial gp60 receptor-based transport and tumor-derived SPARC for targeting, Drug Deliv Rep (2007) 37-41.

[45] M. Simons, An inside view: VEGF receptor trafficking and signaling, Physiology 27(4) (2012) 213-222.

FIGURES

Figure 1: Surface morphology analysis via (A) SEM image (B) AFM image of (a) BSA NPs and (b) AA-GEM-BSA NPs

Figure 2: (I) Confocal images of MCF-7 cells incubated with (A) AA-GEM-BSA NPs, (B) BSA NPs, MDA-MB-231 cells incubated with (C) AA-GEM-BSA NPs, (D) BSA NPs. Panel a and b represents the DAPI stained nucleus and C-6 loaded NPs in the same cells, respectively and panel c reflects the overlay images of panels a and b. Panel d shows a DIC image of the treated cells, and panel e represents high resolution images of panel c. The box analysis (f) line analysis plots (g), and scatter plot analysis (h) show interaction of DAPI and C-6. Scale bar denotes 30 μm. (II) Quantitative cell uptake in (A) MCF-7 and (B) MDA-MB-231 cell lines at concentrations (a) 10 μg/ml, (b) 15 μg/ml and (c) 20 μg/ml.

Figure 3: Intracellular fate of (A) DTX, (B) GEM, (C) DTX+GEM (D) DTX loaded BSA NPs (E) DTX loaded AA-GEM-BSA NPs shown by staining with LysoTracker® Red after 24h. Panel (a) Images under the red fluorescence channel of LysoTracker®; Panel (b) Corresponding differential interface contrast images of cells (c) Superimposition of Panel (a) and Panel (b); Panel (d) and (e) in all the images show vertical and horizontal line series analysis of fluorescence along the white line, respectively.

Figure 4: Apoptosis assay of (A) DTX, (B) GEM, (C) DTX+GEM, (D) AA-GEM-BSA NPs and (E) AA-GEM-BSA NPs against (I) MCF-7 and (II) MDA-MB-231cell lines; (a) green channel depicts the fluorescence from carboxy fluorescein (cell viability marker dye); (b) red channel depicts fluorescence from Annexin Cy3.18 conjugate (cell apoptosis marker dye) (c) represents the overlay image whereas (d) depicts the differential contrast image of representative cells. Scale bar denotes 30 μm.

Figure 5: Plasma concentration-time profiles of Taxotere®, Gemzar®, and NPs following *i.v.* administration in rats

Figure 6: (I) Biochemical markers (A) AST (B) ALT (D) BUN (E) creatinine levels in plasma and (C) MDA level in liver homogenate after 7 days following administration of (b) Gemzar®, (c) Taxotere®, (d) Gemzar® + Taxotere® (e) DTX loaded AA-GEM-BSA NPs as compared to (a) control. Values are expressed as Mean ± SD (n = 5); ***, significant difference at $p < 0.001$, ^{ns}, insignificant and (II) Histopathological sections of (A) kidney, (B) liver and (C) spleen following the treatment with free drugs and NPs

Figure 7: SEM micrographs of RBCs indicative of (A) control and different groups treated with (B) Gemzar®, (C) Taxotere®, (D) Gemzar® + Taxotere®, (E) DTX-AA-GEM-BSA NPs and (F) Hemolytic toxicity of various formulations. Values expressed as Mean ± SD (n = 3).

Figure 8: Fluorescence intensity of (I) C-6 loaded AA-GEM-BSA NPs, (II) Free C-6 in (a) tumor, (b) heart, (c) kidney, (d) liver, (e) lung and (f) spleen and (III) (A) Comparison of % change in tumor volume and (B) % tumor burden of different formulations (***, significant difference at $p < 0.001$, ^{ns}, insignificant) (C) Representative photographs of excised tumors from different treatment groups and (D) Kaplan–Meier survival curve depicting the survival rate of tumor bearing animals received different treatments. The P values are for the log rank test.

TABLES

Table 1: Particle size, PDI and entrapment efficiency of DTX loaded NPs

S. No.	Formulation	Size (diameter in nm)	PDI	Zeta (mV)	% Drug loading	
					DTX	GEM
1.	DTX loaded BSA NPs	139±7	0.13±0.04	-35±2	7.9±0.5	-
2.	DTX loaded AA-GEM-BSA NPs	163±8	0.13±0.09	-27±1	9.1±0.6	3.7±0.2

Values are presented as mean ± SD (n = 6)

Table 2: Pharmacokinetic parameters of Taxotere®, Gemzar®, and NPs following *i.v.* administration

	Parameters				
Samples	C_{30min} (ng/ml h)	$AUC_{(0-24)}$ (ng/ml h)	$AUC_{(0-\infty)}$ (ng/ml h)	$T_{1/2}$ (h)	MRT (h)
Taxotere®	1280±51	3550±76	3970±63	4.2±0.2	4.7±0.4
Gemzar®	1240±70	3670±90	4110±63	4.1±0.6	4.8±0.3
DTX (AA-GEM-BSA NPs)	1130±76	17600±493	24300±534	26±2	37±2
GEM (AA-GEM-BSA NPs)	1000±110	9500±324	15300±476	37±2	50±4

Values are expressed as mean ± SEM (n=5)

*Graphical Abstract

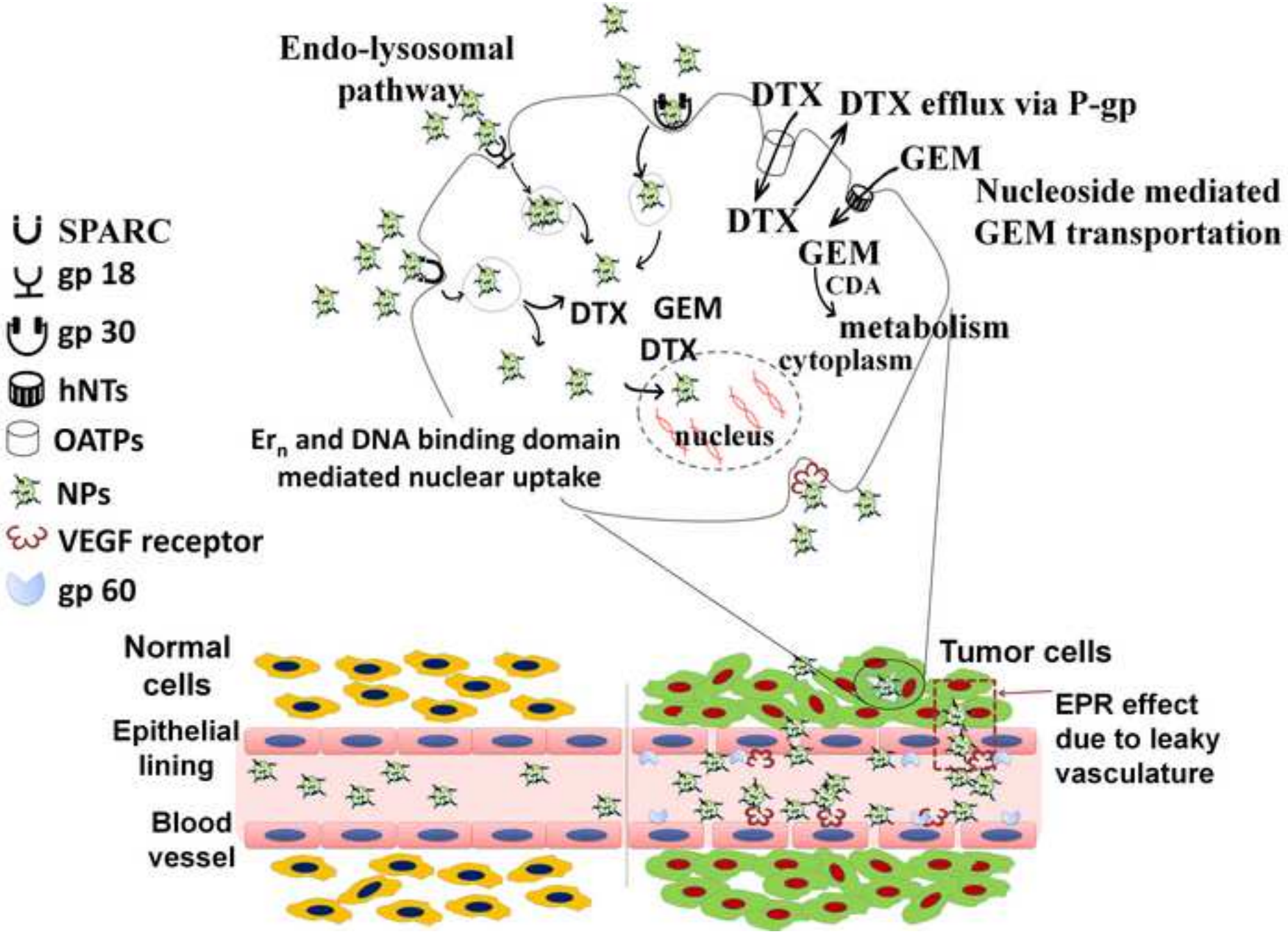

Figure 1

Click here to download high resolution image

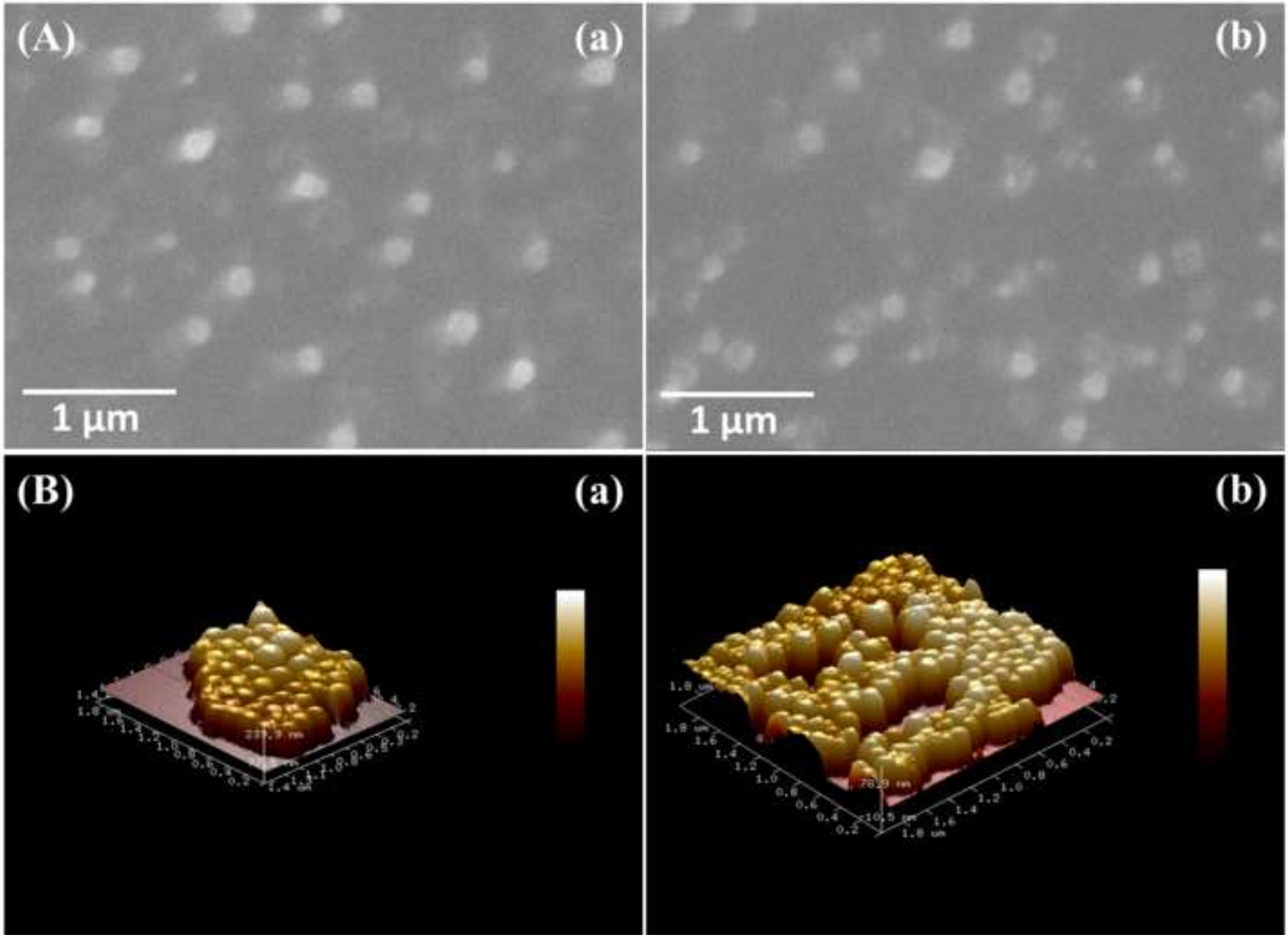

Figure 2

Click here to download high resolution image

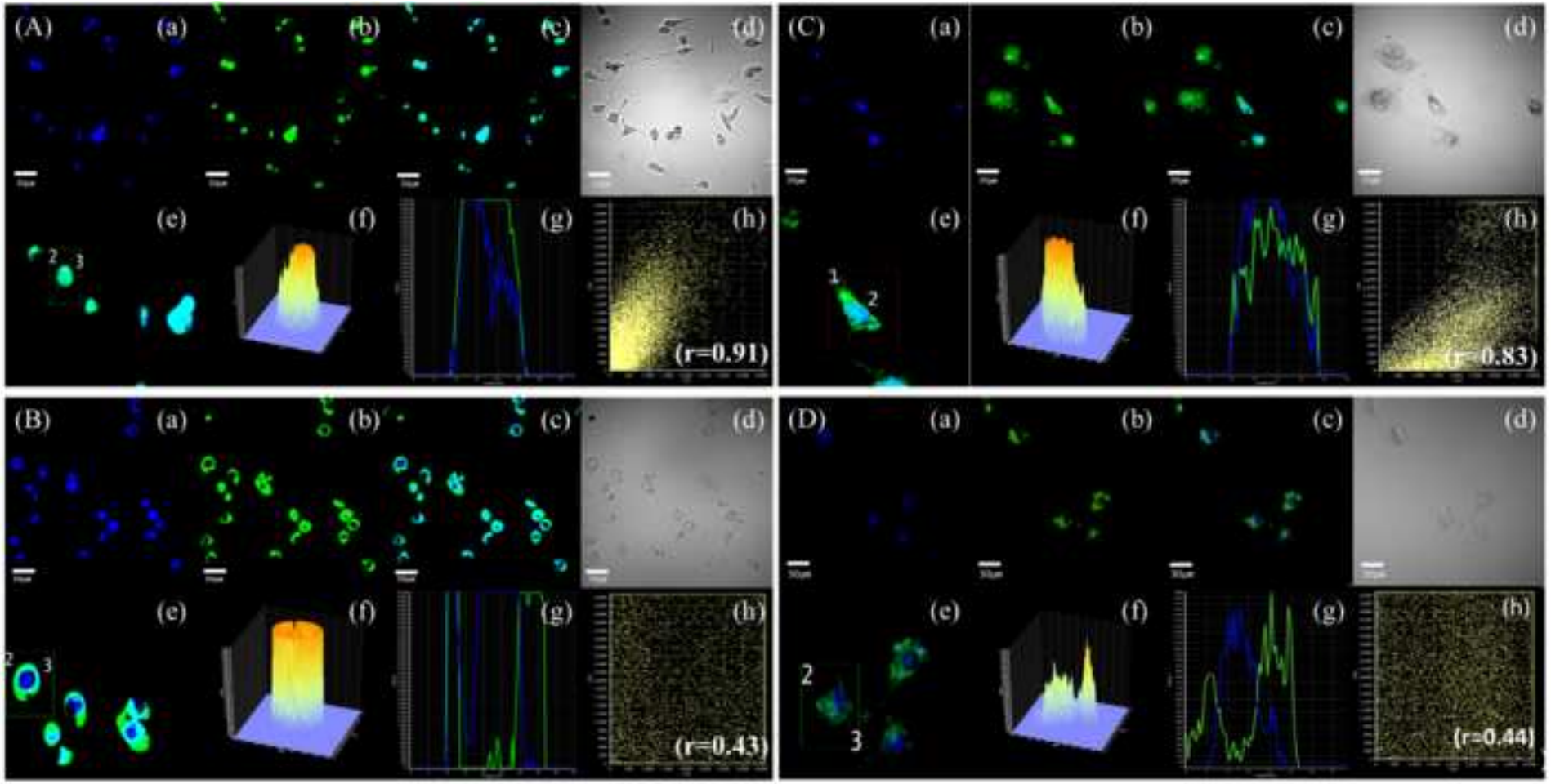

Figure 3

Click here to download high resolution image

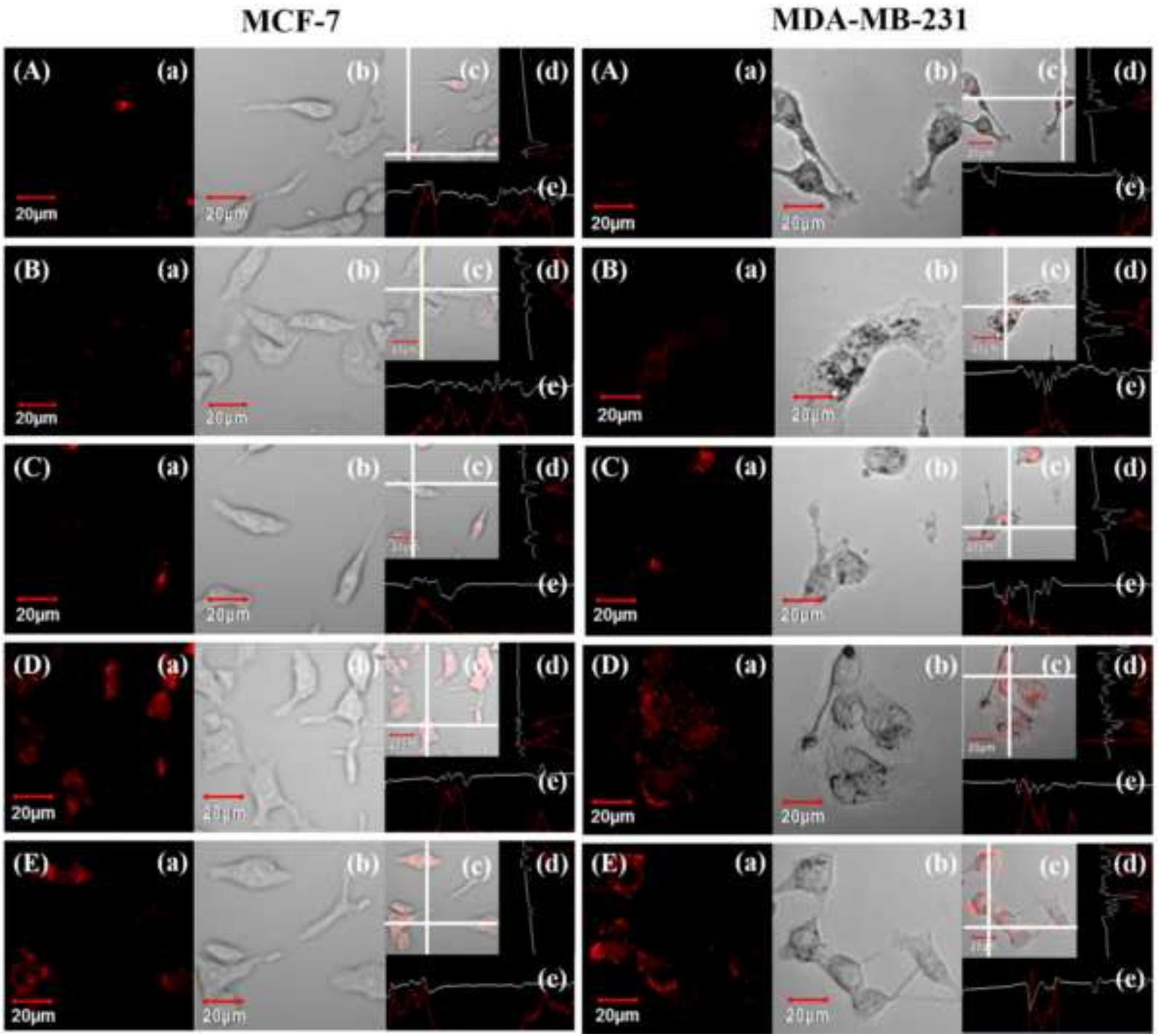

Figure 4

Click here to download high resolution image

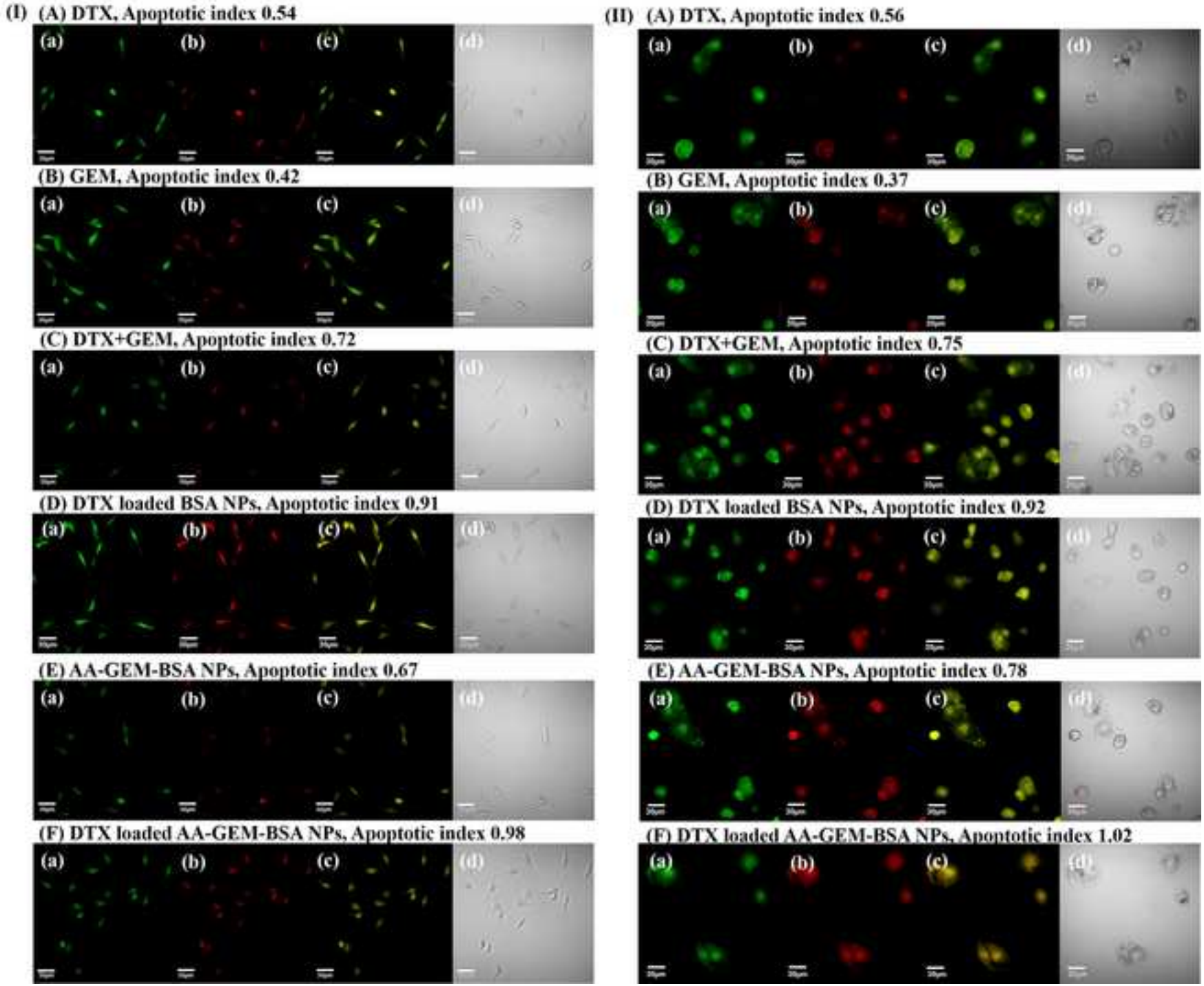

Figure 5

Click here to download high resolution image

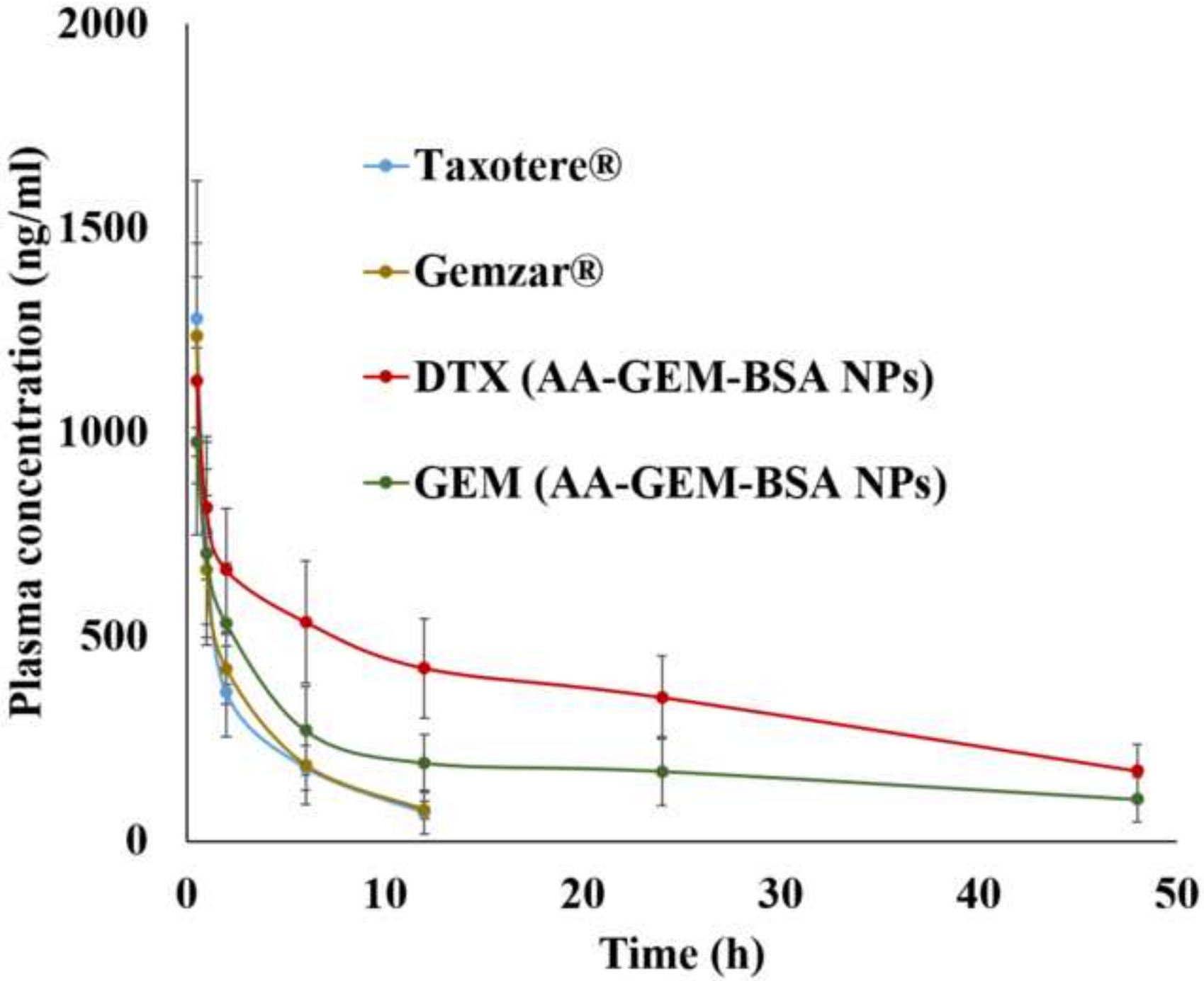

Figure 6

Click here to download high resolution image

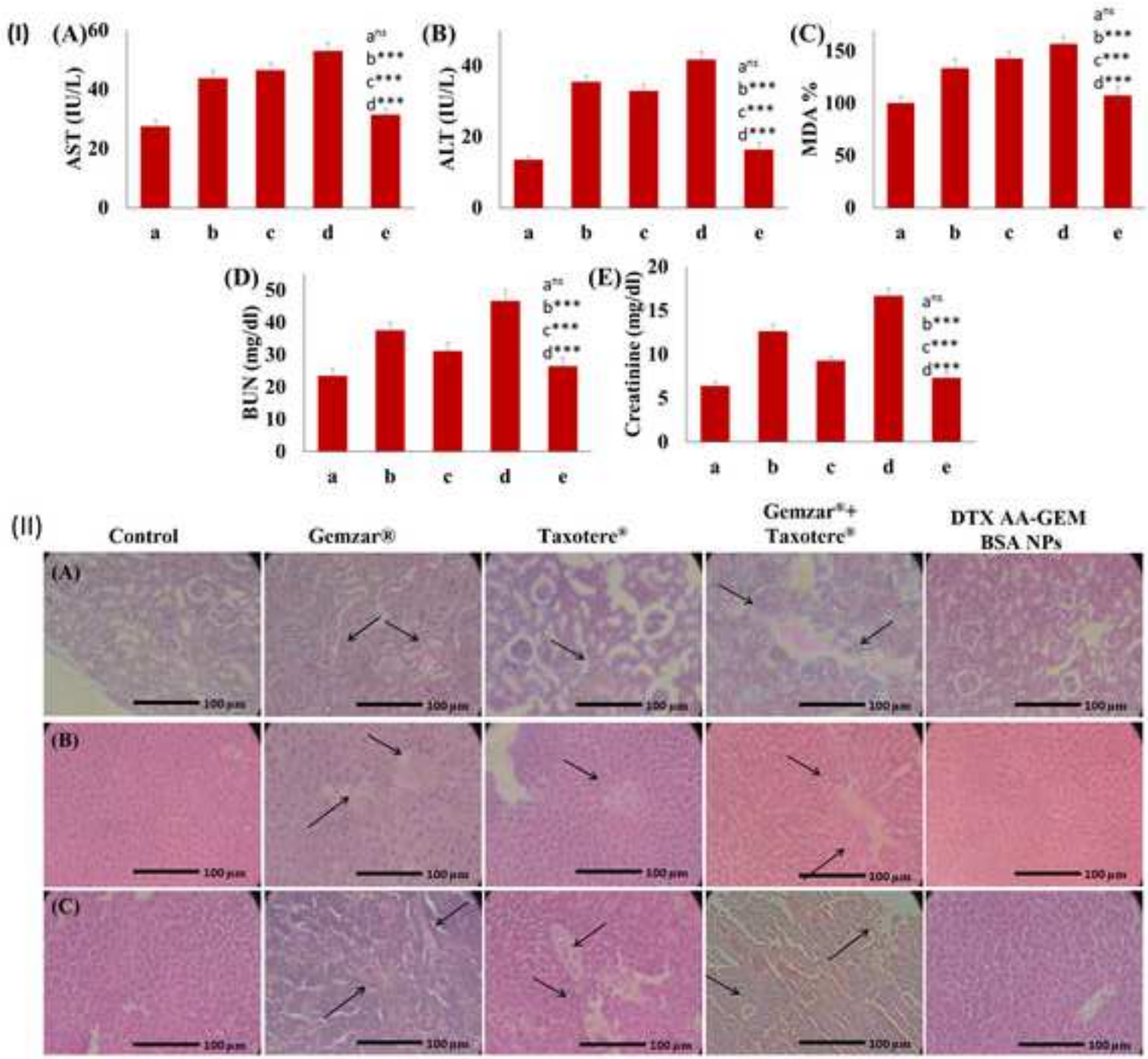

Figure 7

Click here to download high resolution image

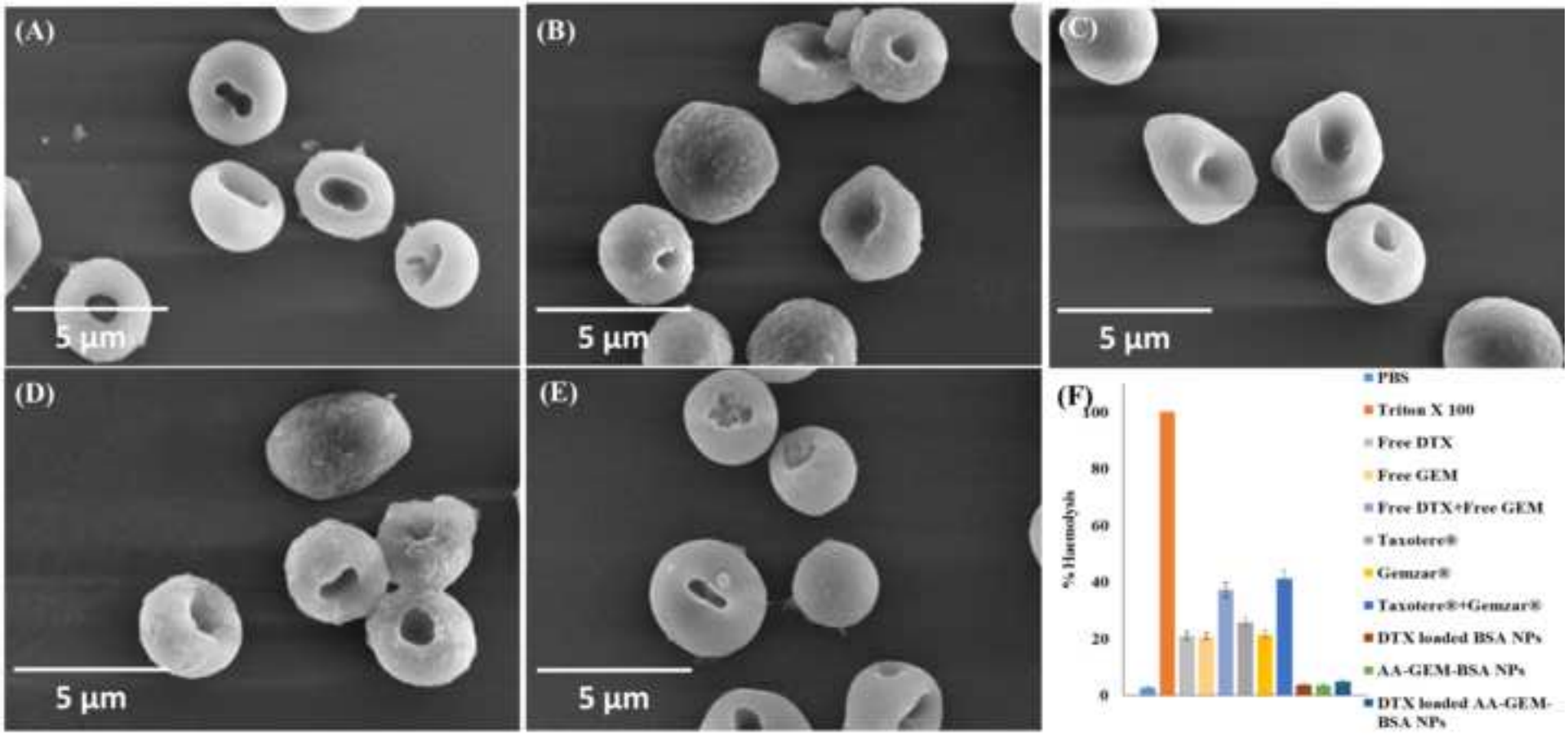

Figure 8

Click here to download high resolution image

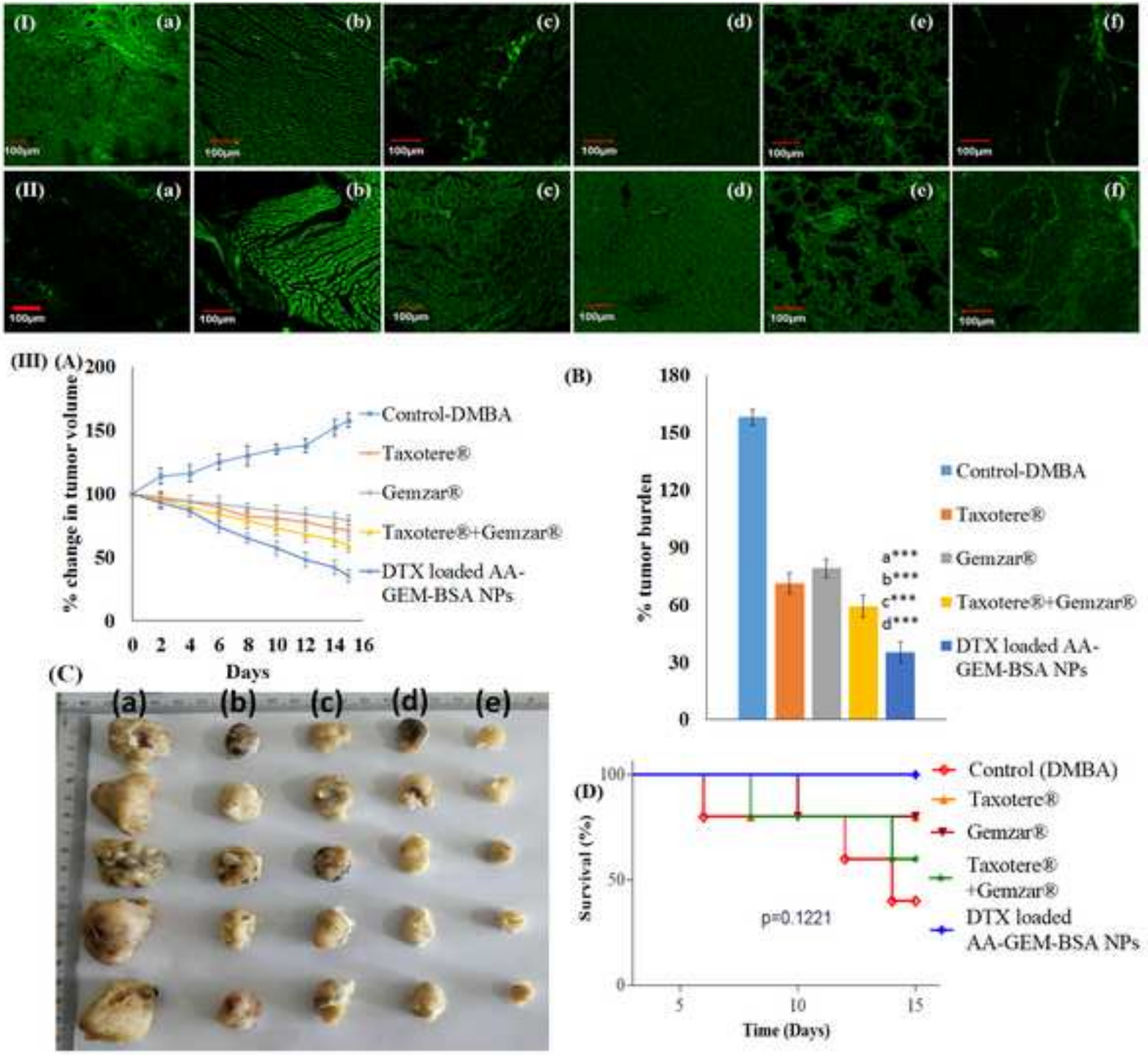

Supplementary Material

Click here to download Supplementary Material: Supplementary Material.docx

Statement of Significance

The present report is the original state of art technology to selectively target dual drug (DTX and GEM) loaded BSA NPs via exploring tumor targeting potential of AA, having high affinity towards VEGF receptors (angiogenesis marker) overexpressed in tumor. The AA and GEM bio-conjugated BSA was synthesized and further used to develop DTX loaded nanoparticles (AA-GEM-BSA NPs). The optimized NPs were further evaluated via extensive in-vitro and in-vivo studies, demonstrating ameliorated cellular uptake, pharmacokinetic and toxicity profile of drugs. Conclusively, DTX loaded AA-GEM-BSA NPs, holds promising potential in increasing the therapeutic efficiency of drugs and overcoming solvent and drug mediated side effects and can be explored further as a scalable platform technology for difficult to deliver drugs.